

CARBON-ENHANCED METAL-POOR STAR FREQUENCIES IN THE GALAXY: CORRECTIONS FOR THE EFFECT OF EVOLUTIONARY STATUS ON CARBON ABUNDANCES

VINICIUS M. PLACCO¹, ANNA FREBEL², TIMOTHY C. BEERS³, RICHARD J. STANCLIFFE⁴

Draft version July 6, 2018

ABSTRACT

We revisit the observed frequencies of Carbon-Enhanced Metal-Poor (CEMP) stars as a function of the metallicity in the Galaxy, using data from the literature with available high-resolution spectroscopy. Our analysis excludes stars exhibiting clear over-abundances of neutron-capture elements, and takes into account the expected depletion of surface carbon abundance that occurs due to CN processing on the upper red-giant branch. This allows for the recovery of the initial carbon abundance of these stars, and thus for an accurate assessment of the frequencies of carbon-enhanced stars. The correction procedure we develop is based on stellar-evolution models, and depends on the surface gravity, $\log g$, of a given star. Our analysis indicates that, for stars with $[\text{Fe}/\text{H}] \leq -2.0$, 20% exhibit $[\text{C}/\text{Fe}] \geq +0.7$. This fraction increases to 43% for $[\text{Fe}/\text{H}] \leq -3.0$ and 81% for $[\text{Fe}/\text{H}] \leq -4.0$, which is higher than have been previously inferred without taking the carbon-abundance correction into account. These CEMP-star frequencies provide important inputs for Galactic and stellar chemical-evolution models, as they constrain the evolution of carbon at early times and the possible formation channels for the CEMP-no stars. We also have developed a public online tool with which carbon corrections using our procedure can be easily obtained.

Keywords: Galaxy: halo—techniques: spectroscopy—stars: abundances—stars: atmospheres—stars: Population II

1. INTRODUCTION

A number of recent studies have shown that Carbon-Enhanced Metal-Poor (CEMP) stars are one of the most important objects for constraining the formation and evolution of the first stellar populations in the Galaxy and the Universe (e.g., Carollo et al. 2012, 2014; Norris et al. 2013b; Cooke & Madau 2014). These stars belong to the broader class of very metal-poor ($\text{VMP} - [\text{Fe}/\text{H}]^5 < -2.0$, e.g., Beers & Christlieb 2005; Frebel & Norris 2013) stars, which have been vigorously searched for and analyzed over the past quarter century. The definition of a CEMP star has been refined over the years, as more high-resolution spectroscopic data has become available, making it possible to distinguish between possible scenarios for their formation. The initial classification by Beers & Christlieb (2005) distinguishes CEMP stars as objects with $[\text{C}/\text{Fe}]$ abundance ratios (or “carbon abundances”, also sometimes referred to as “carbonicity”) at least ten times the solar value ($[\text{C}/\text{Fe}] > +1.0$). However, subsequent analysis has indicated that a more suitable division appears at $[\text{C}/\text{Fe}] \geq +0.7$ (Aoki et al. 2007; Carollo et al. 2012; Norris et al. 2013a).

Generally, CEMP stars in the Galaxy occur over a broad range in both metallicity and carbonicity. The

metallicity, or strictly speaking, the $[\text{Fe}/\text{H}]$ abundance ratio, is commonly used as a proxy for chemical-evolution timescales in the Galaxy. Iron has a very distinctive nucleosynthesis channel (e.g. Woosley & Weaver 1995), and well-traces the enrichment of the interstellar medium through the course of the Galactic evolution. Carbon, on the other hand, has several different formation channels (e.g., Norris et al. 2013b) in the early universe, making it unsuitable for tracing evolutionary timescales. Hence, quantifying the occurrence of CEMP stars as a function of metallicity maps out the evolution of carbon in the early universe.

Broadly speaking, the carbon-enhancement phenomenon can be either *extrinsic* or *intrinsic* to a given star:

Extrinsic enrichment accounts for the observed abundance patterns of the CEMP-s ($[\text{Ba}/\text{Fe}] > +1.0$ and $[\text{Ba}/\text{Eu}] > +0.5$) and CEMP-r/s ($0.0 \leq [\text{Ba}/\text{Fe}] \leq +0.5$) stars (but see Hollek et al. 2014). This pattern is thought to be the result of mass transfer across a binary system, coming from an evolved star that has passed through the asymptotic giant-branch (AGB; e.g., Herwig 2005) evolutionary stage. Radial-velocity monitoring (e.g., Lucciarelli et al. 2005) confirms the binarity of the majority of these CEMP stars, and extensive studies have been conducted to compare the observed abundance patterns with theoretical models (e.g., Bisterzo et al. 2011; Placco et al. 2013; Hollek et al. 2014).

Intrinsic enrichment is thought to be the main formation channel for the CEMP-no ($[\text{Ba}/\text{Fe}] < 0.0$) and CEMP-r ($[\text{Eu}/\text{Fe}] > +1.0$) subclasses of stars. Given that their metallicities are almost exclusively below $[\text{Fe}/\text{H}] = -2.7$ (Aoki et al. 2007), such stars most likely formed from chemically primitive gas clouds. In the case of the CEMP-no stars, there appears to exist a distinct

¹ Gemini Observatory, Hilo, HI 96720, USA

² Department of Physics and Kavli Institute for Astrophysics and Space Research, Massachusetts Institute of Technology, Cambridge, MA 02139, USA

³ Department of Physics and JINA Center for the Evolution of the Elements, University of Notre Dame, Notre Dame, IN 46556, USA

⁴ Argelander-Institut für Astronomie der Universität Bonn, 53121 Bonn, Germany

⁵ $[\text{A}/\text{B}] = \log(N_A/N_B)_* - \log(N_A/N_B)_\odot$, where N is the number density of atoms of a given element in the star (*) and the Sun (○), respectively.

carbon abundance regime where they are found ($\log_{\epsilon}(C) \sim 6.5$; Spite et al. 2013). Contrary to the extrinsically enriched CEMP-s stars, the CEMP-no stars must have formed from carbon-enhanced natal gas clouds. Norris et al. (2013b), and references therein, suggest a number of scenarios for the early production of carbon, and thus the origins of CEMP-no stars. Among these are massive, zero/low-metallicity stars, with/without rotation (Meynet et al. 2006, 2010), and mixing and fallback Type II supernovae, often referred to as “faint supernovae” (Umeda & Nomoto 2005; Tominaga et al. 2007).

One remarkable example of the CEMP-no subclass is BD+44°493 (Ito et al. 2009, 2013; Placco et al. 2014b), a $V = 9$ star with a light-element abundance pattern (e.g., C, N, O, Na, Mg, Al, etc.) that agrees well with yields from faint-supernovae models (Nomoto et al. 2006). Furthermore, observational evidence suggests that the CEMP-no abundance pattern is dominant at low metallicity, given that five of the six stars known to have $[Fe/H] < -4.5$ are CEMP-no stars (Christlieb et al. 2002; Frebel et al. 2005; Norris et al. 2007; Caffau et al. 2011; Hansen et al. 2014; Keller et al. 2014).

In this work, we employ new stellar-evolution models that quantify the changes in surface carbon abundances of metal-poor stars during stellar evolution on the giant branch. We also provide an online tool that allows the calculations of these carbon corrections for a given set of input stellar parameters. After excluding recognized CEMP-s and CEMP-r/s stars, we obtain appropriate corrections to apply to the observed carbon abundances, as a function of the observed $[Fe/H]$ and $\log g$. Proper treatment of the carbon depletion allows for an assessment of the true (intrinsic) CEMP-no stellar frequencies as a function of metallicity. These frequencies, in turn, provide important constraints on Galactic chemical-evolution (e.g., Kobayashi & Nakasato 2011) and population-synthesis models (e.g., Pols et al. 2012), on the initial mass function (IMF; e.g., Lee et al. 2014), and on the chemical compositions of progenitor stellar populations.

This paper is outlined as follows. Section 2 describes the theoretical models used for determining the carbon corrections, followed by details of the data selection in Section 3. Corrections for carbon abundances based on these models are provided in Section 4, including a discussion on the sources of uncertainties in our analysis. We present the corrected carbon abundances for the literature sample in Section 5. Section 6 presents a corrected determination of the cumulative CEMP-star frequencies as a function of metallicity, based on high-resolution spectroscopic analyses reported in the literature. We discuss our results and their astrophysical implications in Section 7.

2. STELLAR-EVOLUTION MODELS

The evolutionary stage of a given star has an impact on the observed carbon (and similarly, nitrogen and oxygen) abundances. During evolution on the upper red-giant branch, carbon from the lower layers of a stellar atmosphere is converted to nitrogen due to the CN cycle, then mixed to the surface of the star, resulting in an increase of the surface nitrogen abundance and reduction in the surface carbon abundance. The amount of carbon depletion depends mostly on the metallicity and

the initial stellar carbon and nitrogen abundances. This effect has already been discussed extensively in the literature (Gratton et al. 2000; Spite et al. 2006; Aoki et al. 2007). However, apart from the CEMP-star classification suggested by Aoki et al. (2007), which takes into account the luminosity of a given star (and hence its evolutionary status), no further investigations have been undertaken to consider the impact of carbon depletion on the giant branch when describing the populations of CEMP stars in Galaxy.

Using the STARS stellar-evolution code (Eggleton 1971; Stancliffe & Eldridge 2009), we have computed a grid of $0.8 M_{\odot}$ stellar-evolution models with a range of initial compositions. We cover four initial metallicities, namely $[Fe/H] = -1.3, -2.3, -3.3$, and -4.3 . For each of these metallicities, we consider a range of initial $[C/Fe]$ values: $[C/Fe] = -0.5, 0.0, +0.5, +0.7, +1.0, +1.5, +2.0, +2.5$ and $+3.0$ ⁶. For $[N/Fe]$, the models are: $[N/Fe] = -0.5, 0.0, +0.5, +0.7, +1.0$, and $+2.0$. In total there are 210 models. Each model is evolved from the pre main-sequence to the tip of the red-giant branch (RGB). It is well-documented that the surface abundances changes occur on the upper part of the RGB (e.g. Gratton et al. 2000) and that some non-convective process is required to account for this. There are many potential mechanisms that can cause this, including (but not limited to) rotation, internal gravity waves, magnetic fields, and thermohaline mixing. For reviews of these mechanisms, we refer the reader to the works of, e.g., Maeder et al. (2013), Mathis et al. (2013), and Stancliffe & Lattanzio (2011).

In this work, to account for extra mixing on the upper giant branch, we follow Stancliffe et al. (2009), who use a diffusive prescription for thermohaline mixing based on the work of Ulrich (1972) and Kippenhahn et al. (1980). This prescription was first shown to reproduce the abundance patterns of red giants by Charbonnel & Zahn (2007), when the one free parameter of the theory⁷ is appropriately chosen. It has been subsequently shown that the same parameter choice reproduces the observed abundance trends across a wide range of metallicities, for both carbon-rich and carbon-normal metal-poor field stars (Stancliffe et al. 2009) and globular-cluster stars (Angelou et al. 2011, 2012). However, it should be noted that hydrodynamical simulations of thermohaline mixing do not support the calibration of the free parameter in use by 1D stellar-evolution codes (see, e.g., Denissenkov & Merryfield 2011). In principle, we must remain open to the possibility that thermohaline mixing is *not* the cause of abundance changes on the giant branch, or that the extent of this mixing is *over-* or *under-*estimated (we further discuss this issue in Section 4.1 with respect to our analysis). In addition, we have not accounted for the role potentially played by the other mixing mechanisms mentioned above. Multidimensional hydrodynamic simulations of envelope convection in red giants (e.g., Viallet et al. 2013) may help to establish the relevant physical

⁶ There are no available models for $[C/Fe] = +3.0$ and $[Fe/H] = -1.3$. Such a substantial carbon enrichment at this metallicity corresponds to a carbon mass fraction of around 0.1, which is implausibly high.

⁷ The free parameter is related to the aspect ratio of the salt fingers responsible for the mixing (see Charbonnel & Zahn 2007, for further details).

mechanism(s) at work.

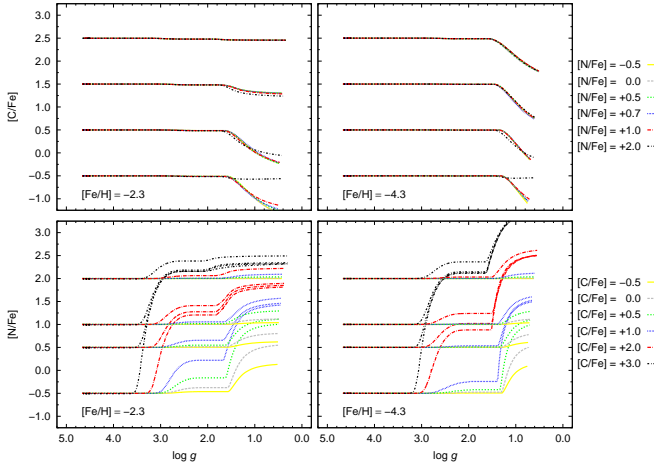


Figure 1. $[C/Fe]$ (upper panels) and $[N/Fe]$ (lower panels), as a function of $\log g$, for models with $[Fe/H] = -2.3$ and $[Fe/H] = -4.3$. The keys on the right side of the plots list the different initial nitrogen and carbon abundances of each model.

Figure 1 shows the behavior of the carbon (upper panels) and nitrogen (lower panels) abundance ratios, as a function of the surface gravity, for a subset of the models with $[Fe/H] = -2.3$ and $[Fe/H] = -4.3$. For $[C/Fe]$, the nitrogen content is largely irrelevant, unless the initial $[C/Fe]$ is very low ($[C/Fe] < 0.0$). The more C- and N-enhanced models appear to deplete more carbon than the less-enhanced ones. This is expected, since these models behave similarly to more metal-rich models, and spend less time on the RGB (see Stancliffe et al. 2009, for further details). For $[N/Fe]$, there is a clear correlation between initial carbon content and the subsequent nitrogen evolution. More initial C leads to larger amounts of N at both first dredge-up and on the upper RGB. This effect becomes less significant as the initial nitrogen content rises.

Using the models described in this Section, it is also possible to see how the C and N abundance ratios relate to each other during the evolution on the RGB. Figure 2 shows the behavior of $[C/Fe]+[N/Fe]$ (upper panel) and $[(C+N)/Fe]$ (lower panel), as a function of $\log g$, for models with $[Fe/H] = -4.3$. We caution that, by simply adding $[C/Fe]$ and $[N/Fe]$, as has sometimes been done in previous work, it is not possible to assess the true level of C+N enhancement, because one cannot differentiate between cases with high C or high N. In some regions the C+N measurement is dominated by C, in some it is dominated by N, and in others the two elements provide similar enhancement.

For a proper treatment of the C+N combination, it is thus necessary to employ $[(C+N)/Fe] = \log [(C+N)/Fe] - \log [(C+N)/Fe]_{\odot}$, i.e., the correct formal definition of $[(C+N)/Fe]$. As expected, this ratio remains almost flat throughout the evolution, given that the total CN content in the star remains unchanged and proton-burning reactions only influence the relative proportions of the CN nuclei. In addition, there are small variations with metallicity, mainly due to extra mixing having less effect at higher metallicities.

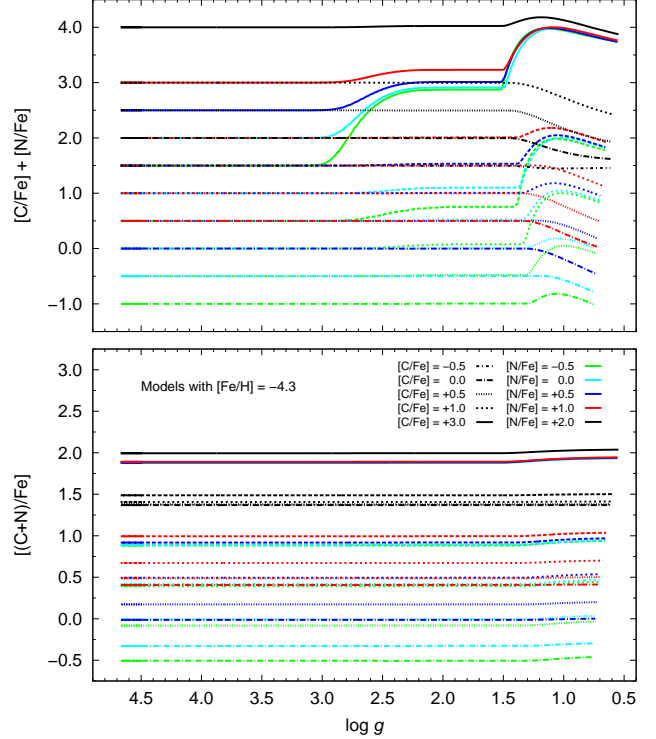


Figure 2. $[C/Fe]+[N/Fe]$ (upper panel) and $[(C+N)/Fe]$ (lower panel), as a function of $\log g$, for a series of models with $[Fe/H] = -4.3$ (see text for definitions). The combinations between different line types and colors give the initial conditions for the 25 models showing in each panel.

3. LITERATURE DATA

For the purpose of determining carbon-abundance corrections, based on stellar-evolutionary status, we attempted to collect all available literature data to select a sample of stars with high-resolution spectroscopic metallicities $[Fe/H] < -1.0$ that have available stellar-atmospheric parameters, along with several critical elemental abundances, including carbon ($[C/Fe]$), nitrogen ($[N/Fe]$), strontium ($[Sr/Fe]$), and barium ($[Ba/Fe]$) abundance ratios, where available. Our sample is based on the most recent version of the SAGA database (Suda et al. 2008) and the compilation of literature data by Frebel et al. (2010). In addition, we collected data from the literature for studies published after these compilations were assembled. Individual references include: Allen et al. (2012), Akerman et al. (2004), Aoki et al. (2002), Aoki et al. (2006), Aoki et al. (2007), Aoki et al. (2008), Aoki et al. (2013), Barklem et al. (2005), Cohen et al. (2008), Cui et al. (2013), Goswami et al. (2006), Gratton et al. (2000), Hansen et al. (2011), Hansen et al. (2014), Hollek et al. (2011), Hollek et al. (2014), Ito et al. (2013), Johnson et al. (2007), Jonsell et al. (2006), Lai et al. (2007), Lai et al. (2008), Masseron et al. (2010), Mashonkina et al. (2012), McWilliam et al. (1995), Meléndez & Barbuy (2002), Placco et al. (2013), Placco et al. (2014a), Preston et al. (2006), Roederer et al. (2008a), Roederer et al. (2010), Roederer et al. (2014), Simmerer et al. (2004), Sivarani et al. (2006), Sneden et al. (2003), Thompson et al. (2008), Yong et al. (2013), and Zhang et al. (2011). The full sample of literature data contains 863 objects, with a total of 792 stars with $[Fe/H] < -1$, $\log g > 0.0$ and $[C/Fe]$ mea-

surements. The only exceptions, where upper limits on carbon were used, are: SDSS J102915 (Caffau et al. 2011), CD-38°245, HE 1424-0241 (Yong et al. 2013), and HE 2239-5019 (Hansen et al. 2014). For consistency, we re-scaled all metallicities and abundances to the Asplund et al. (2009) solar photospheric values.

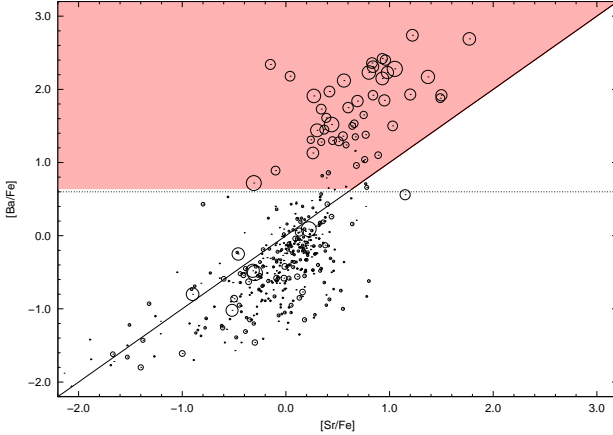


Figure 3. $[\text{Ba}/\text{Fe}]$ vs. $[\text{Sr}/\text{Fe}]$ distribution for the literature sample. The solid line marks the $[\text{Ba}/\text{Sr}] = 0.0$ line, and the dotted line the $[\text{Ba}/\text{Fe}] = +0.6$. The symbol size is proportional to the carbon abundance. The shaded area shows the location of the CEMP-s and CEMP-r/s stars that were excluded from the analysis.

To determine the CEMP-star frequencies as a function of metallicity, known CEMP-s and CEMP-r/s stars should be excluded, since these are believed to be enriched at a later time in their evolution by a now-extinct AGB companion. Besides their enhanced carbon, these objects exhibit a distinct signature of *s*-process elements. Figure 3 shows the behavior of the $[\text{Ba}/\text{Fe}]$ and $[\text{Sr}/\text{Fe}]$ ratios for the literature data. The size of the points is proportional to the star's $[\text{C}/\text{Fe}]$, and the red shaded area marks the location of recognized CEMP-s and CEMP-r/s stars. For the purpose of determining carbon corrections and CEMP stellar frequencies, we excluded stars with $[\text{Ba}/\text{Fe}] > +0.6$ and $[\text{Ba}/\text{Sr}] > 0$ from the subsequent analysis (we studied the effect of changing the criterion to $[\text{Ba}/\text{Fe}] > +0.8$ on the calculated cumulative CEMP-star frequencies, and results are given in Section 6).

Ideally, only stars with actual $[\text{Ba}/\text{Fe}]$ and $[\text{Sr}/\text{Fe}]$ measurements should be used to determine the CEMP-star frequencies. However, it is possible to include stars with upper limits on $[\text{Ba}/\text{Fe}]$ that indicate $[\text{Ba}/\text{Fe}] < 0$, and also to assess the level of “contamination” from CEMP-s and CEMP-r/s stars without $[\text{Ba}/\text{Fe}]$ and $[\text{Sr}/\text{Fe}]$ measurements. From the 792 stars selected above, 665 exhibit $[\text{Ba}/\text{Fe}] < +0.6$, upper limits for $[\text{Ba}/\text{Fe}]$, or no $[\text{Ba}/\text{Fe}]$ measurements. Within this selected sample, 505 stars have $[\text{Fe}/\text{H}] \leq -2.0$, which is the metallicity range used for the CEMP-star frequency calculations. There are 87 stars without $[\text{Ba}/\text{Fe}]$ measurements, and 22 with only upper limits (only 5 upper limits are greater than $[\text{Ba}/\text{Fe}] > +0.6^8$). Out of these 66 stars, 40 have either

⁸ These are: HE 1327-2326 (Frebel et al. 2005), SDSS J2209-0028 (Spite et al. 2013), G 77-61 (Masseron et al. 2012), HE 0107-5240 (Christlieb et al. 2004), and HE 0233-0343 Hansen et al. (2014), which are all well-known CEMP-no stars with $[\text{Fe}/\text{H}] \leq -4.0$.

$[\text{Sr}/\text{Fe}] \geq +0.3$ (the typical lower limit for CEMP-s and -r/s stars; Frebel & Norris 2013) or no Sr abundances measured. Assuming that all 40 stars mentioned above were CEMP-s or -r/s, and were mistakenly added to the CEMP-star frequency calculations, they would account for 8% of the total sample (505 stars). However, since the sample has no selection bias on carbon, we would expect a contribution of between 10-20% by CEMP-s or -r/s stars, meaning that no more than $\sim 2\%$ of the selected 505 star sample is contaminated. This fraction could be even lower, since the CEMP-s and CEMP-r/s are more prevalent in the $[\text{Fe}/\text{H}] > -3.0$ range.

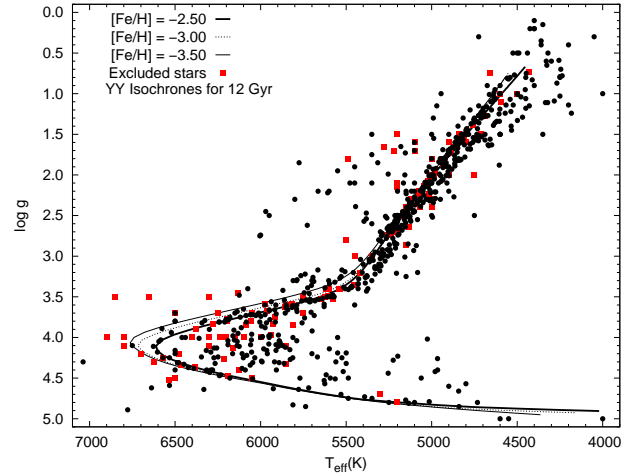


Figure 4. H-R diagram for the literature stars. The black filled circles are the dataset used for the determination of the CEMP-star frequencies, and the red filled squares are the excluded CEMP-s and CEMP-r/s stars. Overplotted are the Yale-Yonsei isochrones (Demarque et al. 2004) for ages of 12 Gyr and 3 different values of $[\text{Fe}/\text{H}]$.

Figure 4 shows the behavior of T_{eff} and $\log g$ for the literature sample, compared with 12 Gyr Yale-Yonsei Isochrones (Demarque et al. 2004) for $[\text{Fe}/\text{H}] = -3.5$, -3.0 , and -2.5 . The CEMP-s and CEMP-r/s stars, which were excluded from the CEMP-star frequency calculations, are also shown. It is possible to see that the bulk of the sample exhibits $\log g < 2.5$, which is the range where the carbon corrections are applied (see Section 4 for further details). In order to establish corrections for $[\text{C}/\text{Fe}]$ and the frequencies of CEMP stars as a function of metallicity, we used the 505 stars falling outside the shaded area on Figure 3. Figure 5 shows the distribution of carbon abundances, as a function of metallicity, for the literature sample. The symbols are the same as Figure 4. The side panels show the marginal distributions of $[\text{C}/\text{Fe}]$ and $[\text{Fe}/\text{H}]$ for the selected stars. As expected, the CEMP-s and CEMP-r/s stars are mostly concentrated at $[\text{Fe}/\text{H}] > -3.0$ and $[\text{C}/\text{Fe}] > +1.0$.

Figure 6 shows the carbon abundances, as a function of $\log g$, for the 505 selected stars divided in $[\text{Fe}/\text{H}]$ bins bracketing the model values. Also shown are the models described in Section 2, assuming an initial nitrogen abundance of $[\text{N}/\text{Fe}] = 0.0$ (see Section 4.3 for further details). One can see that a number of stars fall outside the $\log g$ range of the theoretical models. In these cases, we used the corrections for the last $\log g$ model value as a constant for all $\log g$ outside the model range, instead of a

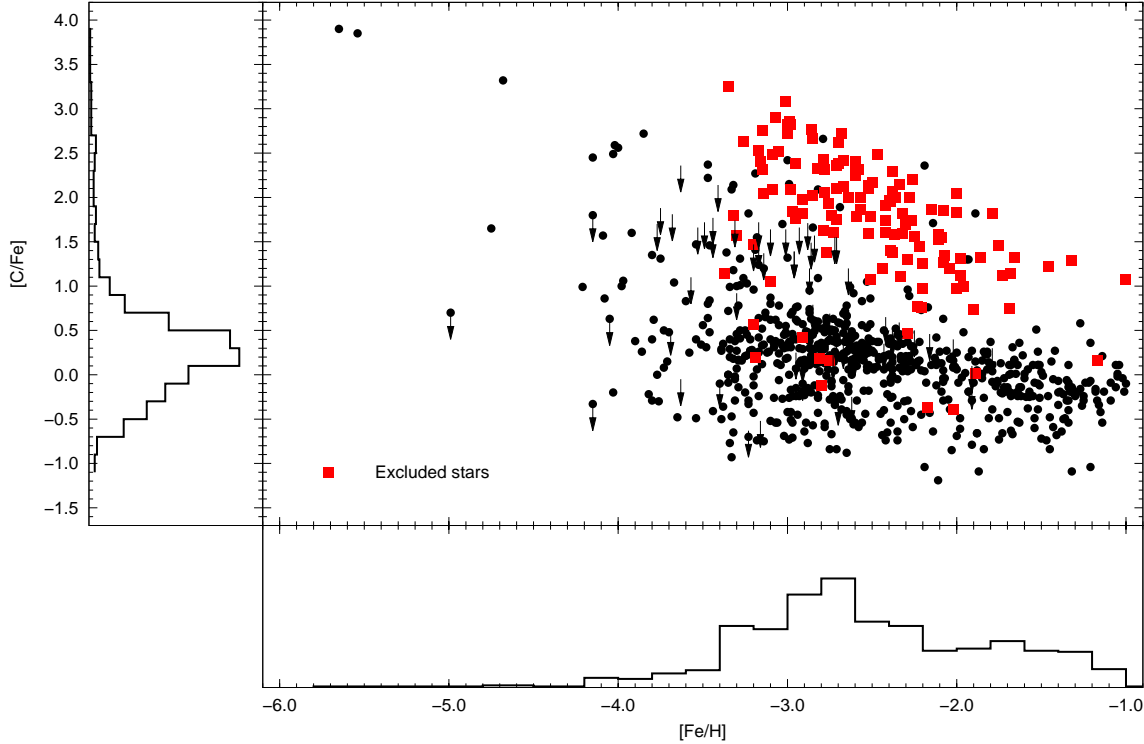


Figure 5. $[C/Fe]$, as a function of metallicity, $[Fe/H]$, for the literature stars with available measurements. The black filled dots are the accepted stars, and the red filled squares are CEMP-s and CEMP-*r/s* stars that were excluded from the analysis. The marginal distributions of each variable for the accepted stars are shown as histograms.

linear extrapolation that could lead to an over-estimation of the carbon corrections. The following section provides a detailed explanation of this procedure.

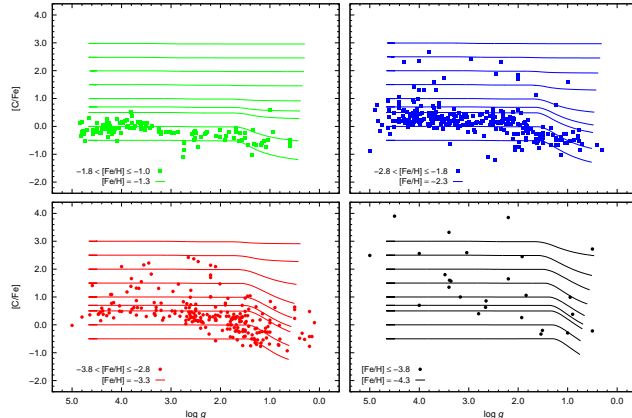


Figure 6. Carbonicities, $[C/Fe]$, for the literature data, as a function of $\log g$, divided into four $[Fe/H]$ ranges. The horizontal solid lines are the models with $[N/Fe]=0.0$.

4. CORRECTIONS FOR $[C/Fe]$

In this section we present our procedure to determine corrections for the observed carbon abundances of CEMP stars, based on their evolutionary status, using the theoretical models described in Section 2. We also discuss possible effects of the uncertainties in the atmospheric parameters and the choice of initial $[C/Fe]$ and $[N/Fe]$ abundances on the derived corrections.

4.1. Further Considerations on the Stellar-Evolutionary Models

Before proceeding to the determination of the carbon-abundance corrections, it is worth noticing a slight mismatch between the behavior of depletion in the theoretical models and the observations seen in Figure 6, in particular in the top-right panel. The model tracks and the data should show the same decrease in $[C/Fe]$ with decreasing $\log g$ (for $\log g < 2.0$). From the figure it appears, however, that the onset of the mixing mechanism in the models is somewhat “delayed” in $\log g$ space, and only occurs at lower $\log g$ values than the data suggests. This effect is more noticeable for stars with $[C/Fe] < +0.7$. This offset prevents a proper estimate of the amount of depleted carbon. The $[C/Fe]$ corrections would be under-estimated by the models, as would the CEMP-star frequencies. To account for this, we introduce a shift in $\log g$ on the models before calculating the corrections for $[C/Fe]$. Such a shift should lead to a constant average $[C/Fe]$ as a function of $\log g$ after the abundance corrections are applied.

To test this hypothesis, we calculated the corrections for the carbon abundances for three $\log g$ offsets (using the procedure described below in Section 4.2): (i) original model $\log g$ only; (ii) model $\log g + 0.3$ dex and; (iii) model $\log g + 0.5$ dex. Results are shown in Figure 7. One can see that corrections based solely on the original models (Panel b) are not sufficient to recover the depleted carbon on the upper-RGB ($\log g < 2$), whereas the shifted models, with an early mixing onset, are able to keep the $[C/Fe]$ values constant over the entire $\log g$ range. Even though the corrections for case (ii) improve

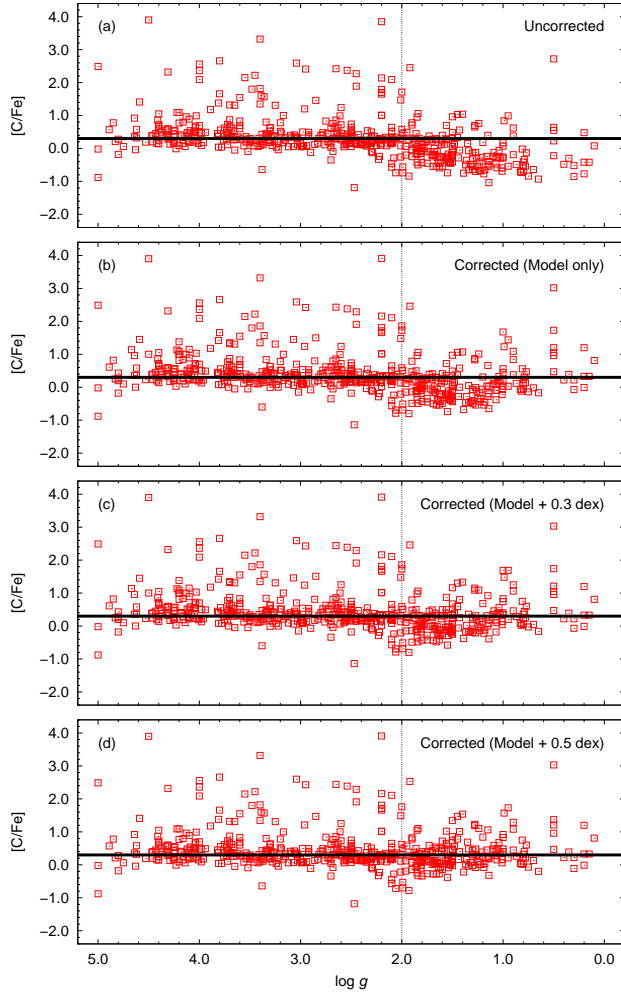


Figure 7. $[C/Fe]$ as a function of $\log g$ for the literature sample. Panel (a): Observed carbon abundances. Panel (b): $[C/Fe]$ corrected with the original models only. Panel (c): $[C/Fe]$ corrected with model $\log g + 0.3$ dex shift. Panel (d): $[C/Fe]$ corrected with model $\log g + 0.5$ dex shift. The solid horizontal line represents a constant $[C/Fe]=+0.3$ value to guide the eye. The vertical dashed line is a reference line at $\log g = 2.0$.

the behavior of the corrected carbon abundances, there is still a decrease in the distribution for $\log g < 2$ (Panel c). Hence, we proceed with the $+0.5$ dex correction, shown in Panel (d). The effect of these corrections on the $[C/Fe]$ averages are described in Section 5. We also quantify the effect of the $\log g$ shift on the CEMP-star frequencies, as described in Section 6.

4.2. Procedure

Since the initial carbon abundance of a given star (at least one that has evolved past the first dredge-up) is a-priori unknown, we cannot match the observed abundance with the *initial* abundance of the model as a first approximation. To deal with this issue (we discuss further implications in Section 4.3), we developed a simple procedure to estimate the amount of carbon depletion for a given set of stellar parameters and carbon abundance, without any assumption on the initial carbon abundance.

For a given set of $[Fe/H]$, $[C/Fe]$, and $\log g$, we first identify the two closest model metallicities and, for each of these, we find the two models with the closest ($\log g, [C/Fe]$) values to the input. Then, for each of the

four chosen models, a correction is determined by the difference between the initial $[C/Fe]$ of the model and the $[C/Fe]$ value for the given $\log g$. The final $[C/Fe]$ correction for the input value is then given by a linear interpolation (in $[Fe/H]$ and $[C/Fe]$) of the four model corrections. This process is repeated for each initial $[N/Fe]$ value. In Section 4.3 we discuss the $[N/Fe]$ model choices and uncertainties in detail.

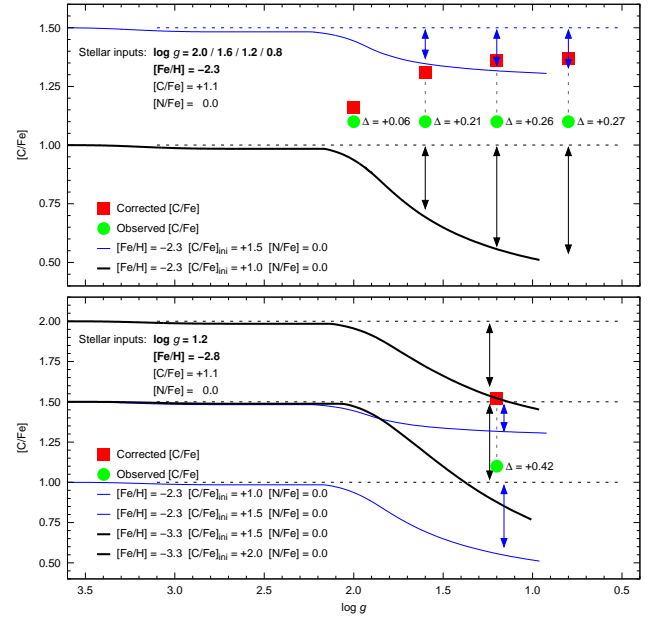


Figure 8. Procedure for the determination of carbon-abundance corrections. Top panel: Observed (green circles) and corrected (red squares) carbon abundances for four different $\log g$ values. The horizontal dashed lines show the initial $[C/Fe]$ model values. The final corrections, Δ , are determined from a linear interpolation of the corrections of each model (vertical arrows). Since the $[Fe/H]$ input value coincides with the model values, no interpolation in $[Fe/H]$ is made. Bottom panel: Complete interpolation procedure for $\log g = 1.2$, and $[Fe/H] = -2.8$. The four vertical arrows represent the corrections for each model. The final correction is a linear interpolation in both $[Fe/H]$ and $\log g$.

As an example, consider the following input observed parameters: $\log g = 1.3$, $[Fe/H] = -3.0$, and $[C/Fe] = +1.0$ (considering a fixed $[N/Fe] = 0.0$). The two closest model metallicities are $[Fe/H] = -2.3$ and -3.3 . For $\log g = 0.8$ and $[C/Fe] = +1.0$, the closest *initial* model carbon abundances are $[C/Fe] = +1.0$ (M1) and $+1.5$ (M2) for the $[Fe/H] = -2.3$ model, and $[C/Fe] = +1.5$ (M3) and $+2.0$ (M4) for the $[Fe/H] = -3.0$ model. For each of the four models, a correction is determined: $\Delta_{M1} = +0.42$ dex, $\Delta_{M2} = +0.18$ dex, $\Delta_{M3} = +0.56$ dex, and $\Delta_{M4} = +0.44$ dex. The final interpolated correction is $\Delta = +0.47$ dex.

Figure 8 illustrates this procedure. The top panel shows four different $\log g$ values, with fixed $[Fe/H] = -2.3$, $[C/Fe] = +1.1$, and $[N/Fe] = 0.0$. For clarity, we chose an input $[Fe/H]$ value that matches one of the models, so the interpolation is performed only between models with different initial carbon abundances. The horizontal dashed lines show the initial $[C/Fe]$ model values, and the vertical arrows represent the amount of carbon depleted for a given $\log g$ value, which corresponds to the carbon correction. The double-headed arrows represent the correc-

tions for each selected model, and the Δ values are the final interpolated corrections for each $\log g$ value.

The bottom panel of Figure 8 shows the complete procedure for determining the carbon correction, for a star with $[\text{Fe}/\text{H}] = -2.8$, $[\text{C}/\text{Fe}] = +1.1$, $[\text{N}/\text{Fe}] = 0.0$, and $\log g = 1.2$. The solid lines are the four models chosen for the interpolation, and the dashed lines show the initial carbon abundance of the models. The final correction is given by a linear interpolation of the four individual corrections, in the $[\text{Fe}/\text{H}]$ vs. $[\text{C}/\text{Fe}]$ plane. It is worth noting from the bottom panel of Figure 8 that, depending on the metallicity, the initial $[\text{C}/\text{Fe}]$ choices change. In this example, the $[\text{Fe}/\text{H}] = -2.3$ models have initial $[\text{C}/\text{Fe}]$ of +1.0 and +1.5, while the $[\text{Fe}/\text{H}] = -3.3$ models have initial $[\text{C}/\text{Fe}]$ of +1.5 and +2.0. This is just a reflection of the fact that, for a given $\log g$ and $[\text{C}/\text{Fe}]$, the amount of carbon depletion increases with decreasing metallicity.

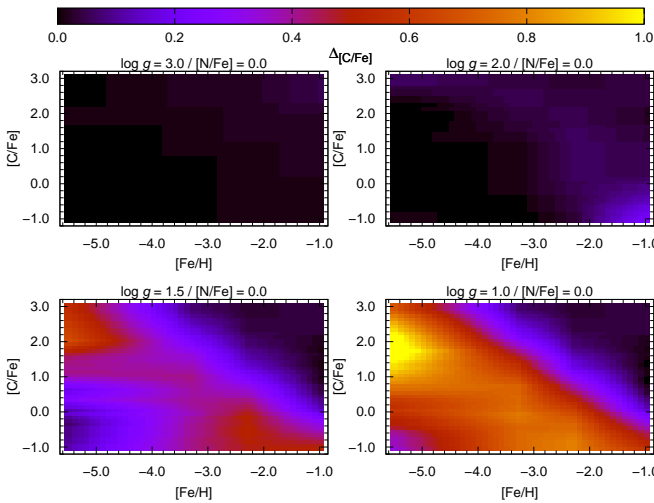


Figure 9. $[\text{C}/\text{Fe}]$ correction map for $\log g = 3.0, 2.0, 1.5$, and 1.0 .

By choosing the interpolation instead of fixed bins in $[\text{Fe}/\text{H}]$ and $[\text{C}/\text{Fe}]$, the corrections exhibit a smooth transition throughout the parameter space. Figure 9 shows a map of the calculated corrections in the $[\text{Fe}/\text{H}]$ vs. $[\text{C}/\text{Fe}]$ plane, for four different $\log g$ values and $[\text{N}/\text{Fe}] = 0.0$. For $\log g = 1.0$, the corrections can be as high as +1.0 dex for $[\text{C}/\text{Fe}] = +2.0$ and $[\text{Fe}/\text{H}] < -5.0$. In contrast, the corrections do not exceed +0.25 dex for $\log g = 2.0$, and are almost non-existent ($\Delta < +0.05$ dex) for $\log g = 3.0$. This is physically reasonable – carbon is little affected by the action of first dredge-up, and is only substantially depleted on the upper part of the RGB. We have developed and made available an online tool⁹, which allows the user to calculate the carbon corrections for a given set of stellar parameters.

4.3. Uncertainties

The two main factors that can affect the determination of the carbon-abundance corrections are the choice of an appropriate model (based on $[\text{Fe}/\text{H}]$, initial $[\text{C}/\text{Fe}]$, and $[\text{N}/\text{Fe}]$), and the uncertainties associated with the input $\log g$ values. We discuss these issues below.

⁹ <http://staff.gemini.edu/~vplacco/carbon-cor.html>

4.3.1. Choice of Model

The model choice itself results in two sources of uncertainties: (i) the observational uncertainties associated with the carbon abundances and metallicity determinations, and (ii) the choice of the correct initial $[\text{N}/\text{Fe}]$, when the observed value is not available. The interpolation procedure described above somewhat minimizes these effects, but below we provide estimates that can be used as guidelines on the uncertainties of the carbon corrections.

In order to quantify how the corrections would change, given the uncertainties associated with the observational determinations of $[\text{Fe}/\text{H}]$ and $[\text{C}/\text{Fe}]$, we calculated the carbon corrections (assuming fixed $\log g = 3.0/2.0/1.5/1.0$ and $[\text{N}/\text{Fe}] = 0.0$), for a series of $[\text{Fe}/\text{H}]$ and $[\text{C}/\text{Fe}]$ combinations, in steps of 0.25 dex, with $[\text{Fe}/\text{H}]$ ranging from -4.0 to -2.0 , and $[\text{C}/\text{Fe}]$ from 0.0 to $+2.0$. The size step of 0.25 dex is similar to the total uncertainty associated with measurements of $[\text{Fe}/\text{H}]$ and $[\text{C}/\text{Fe}]$.

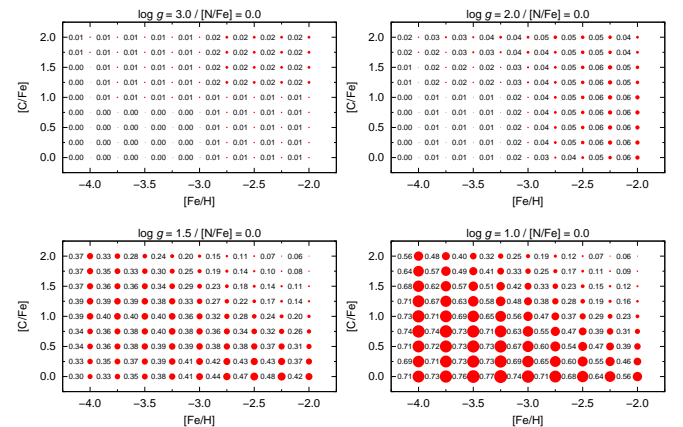


Figure 10. Carbon-abundance corrections for $\log g = 3.0, 2.0, 1.5$, and 1.0 , assuming $[\text{N}/\text{Fe}] = 0.0$ as the initial nitrogen abundance. The size of each point is proportional to the correction value, which is shown on the left side of each symbol. The step size is 0.25 dex in both $[\text{Fe}/\text{H}]$ and $[\text{C}/\text{Fe}]$.

Figure 10 shows the result of this exercise. Each panel shows the corrections for different $\log g$ values, where the size of the points are proportional to the numbers shown on the left side of each point. As already mentioned, the corrections would be mostly affected by uncertainties in the measured parameters for $\log g \leq 1.0$. For example, a star with $\log g = 1.0$, $[\text{Fe}/\text{H}] = -3.0$, and $[\text{C}/\text{Fe}] = +1.0$ has a determined correction of +0.56 dex. Assuming an uncertainty of ± 0.25 dex in $[\text{C}/\text{Fe}]$, the corrections would vary from +0.48 dex to +0.63 dex (−0.08 dex and +0.07 dex from the calculated value). For $\log g = 1.5$, the corrections would change by −0.03 dex and +0.02 dex, and for $\log g = 2.0$ the corrections would change by no more than ± 0.01 dex. A similar exercise can be performed for $[\text{Fe}/\text{H}]$, even though the uncertainties of its measurement based on high-resolution spectra are often on the order of ± 0.10 dex or less.

Nitrogen abundances are much more challenging to determine in the optical spectra of metal-poor stars. The CN band at 3883 Å can be used if available (assuming a fixed carbon abundance – Placco et al. 2013), or better,

the NH molecular feature at 3360 Å (Placco et al. 2014a). Since a large number of our literature-sample stars lack determinations of nitrogen abundances, we studied the effect of a poor choice of initial [N/Fe] on the carbon corrections. As seen in Figure 1, the corrections are higher for models with low initial carbon abundance and high initial nitrogen abundance. One possibility to assess if this would be a possible physical scenario is by looking at the distribution of [C/Fe] as a function of [N/Fe] for stars that did not evolve through the RGB. Results are shown in Figure 11.

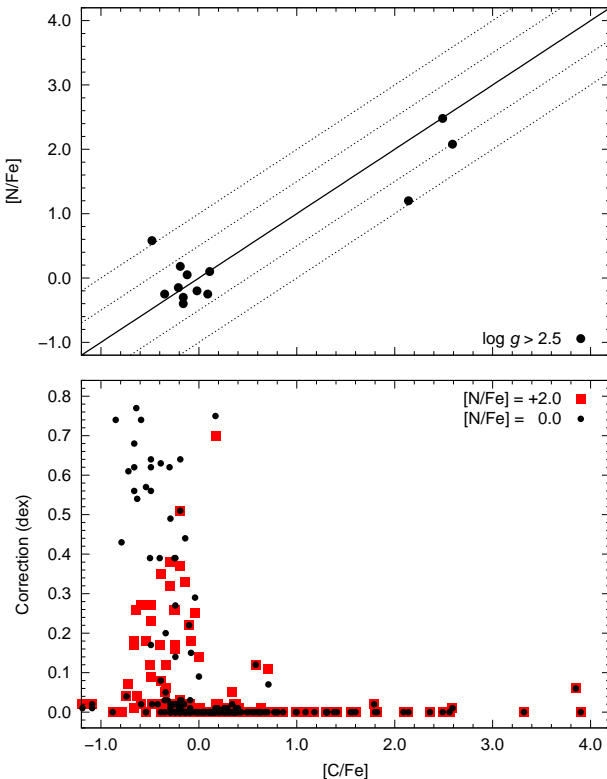


Figure 11. Top panel: $[N/Fe]$ vs. $[C/Fe]$ for the literature stars with $\log g > 2.5$ and available carbon and nitrogen abundances. The solid line is $[C/N] = 0$, and the dotted lines $[C/N] = -1.0/-0.5/0.5/1.0$. Bottom panel: Comparison between the carbon corrections as a function of $[C/Fe]$ for the $[N/Fe] = 0.0$ (black filled circles) and $[N/Fe] = +2.0$ (red filled squares) models.

The upper panel of Figure 11 shows the behavior of high-resolution $[N/Fe]$ vs. $[C/Fe]$ measurements for stars with $\log g > 2.5$. One can see that the majority of the stars are within ± 0.5 dex from the $[N/Fe] = [C/Fe]$ line. This suggests that a good approximation for the initial nitrogen abundance could be the same value as the carbon abundance. The lower panel of Figure 11 shows the carbon corrections for the $[N/Fe] = 0.0$ and $[N/Fe] = +2.0$ models, for stars with measured nitrogen abundances. As expected from the models, the corrections are larger when both carbon and nitrogen abundances are low, and are negligible for stars with $[C/Fe] > +2.0$. Since the choice of initial $[N/Fe]$ seems to affect mostly the stars with lower $[C/Fe]$, we chose, for simplicity, the $[N/Fe] = 0.0$ model for the determination of the CEMP-star frequencies in Section 6. Moreover, since there are no large differences in the carbon corrections between the nitro-

gen models for $[C/Fe] \geq +0.5$, this will not affect the CEMP-star frequencies calculations discussed below.

4.3.2. Uncertainty in $\log g$

An additional source of uncertainty on the carbon-correction determination is the one associated with the measured surface gravity, $\log g$. This is a combination of the uncertainty in the model atmosphere, and on the ability to reliably measure Fe I and Fe II lines in the spectra, which is particularly challenging for stars with $[Fe/H] < -3.0$, even in high-resolution. For the carbon-correction determinations, this uncertainty has a greater impact for stars with $\log g \leq 2.2$, assuming a typical uncertainty of ~ 0.3 dex. To evaluate the extent of the $\log g$ uncertainty on the $[C/Fe]$ correction, we calculated the corrections for a small grid of $[C/Fe]$ and $\log g$ values, assuming $[Fe/H] = -2.5$ and $[N/Fe] = 0.0$. Then, for each case, we then redetermined the corrections for two additional cases: $\log g + 0.30$ and $\log g - 0.30$.

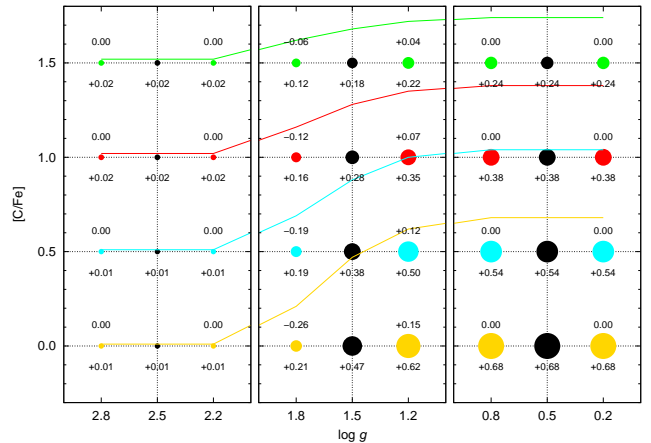


Figure 12. Changes in carbon-abundance corrections as a function of $\log g$. The black filled circles, crossed by the dotted lines, are the grid values, with two colored points at $\log g \pm 0.3$. Each color represents a different initial $[C/Fe]$. The values below the points are the $[C/Fe]$ corrections using $[N/Fe] = 0.00$, and the values above the points are difference in the carbon correction from the grid value. The colored solid lines show the corrected $[C/Fe]$ for the circles along the horizontal dotted lines. The size of each point is proportional to the $[C/Fe]$ correction.

Figure 12 shows how these changes in $\log g$ affect the carbon-abundance corrections. The black circles crossed by the dotted lines represent the grid points, and the filled circles at ± 0.30 dex in $\log g$ show the changes in the carbon corrections. The numbers below each symbol are the difference between the correction for the shifted $\log g$ value and the grid point, and the solid lines show the corrected $[C/Fe]$ for each point, matched by its color. For example, for a star with measured $[Fe/H] = -2.5$, $[C/Fe] = +1.0$ and $\log g = 1.5$, the calculated $[C/Fe]$ correction for $[N/Fe] = 0.0$ is $+0.28$ dex. Assuming a ± 0.3 dex uncertainty in $\log g$, the correction value would vary between $+0.16$ dex and $+0.35$ dex. For a measured $\log g = 2.5$, the corrections would not vary.

As expected, uncertainties of up to ± 0.5 dex in $\log g$ for stars in the $\log g > 3.0$ regime will not have any effect on the derived corrections. For the $\log g = 0.5$ case, the shifts in $\log g$ produce no deviations, since $\log g$ values outside the shifted model range assume a constant cor-

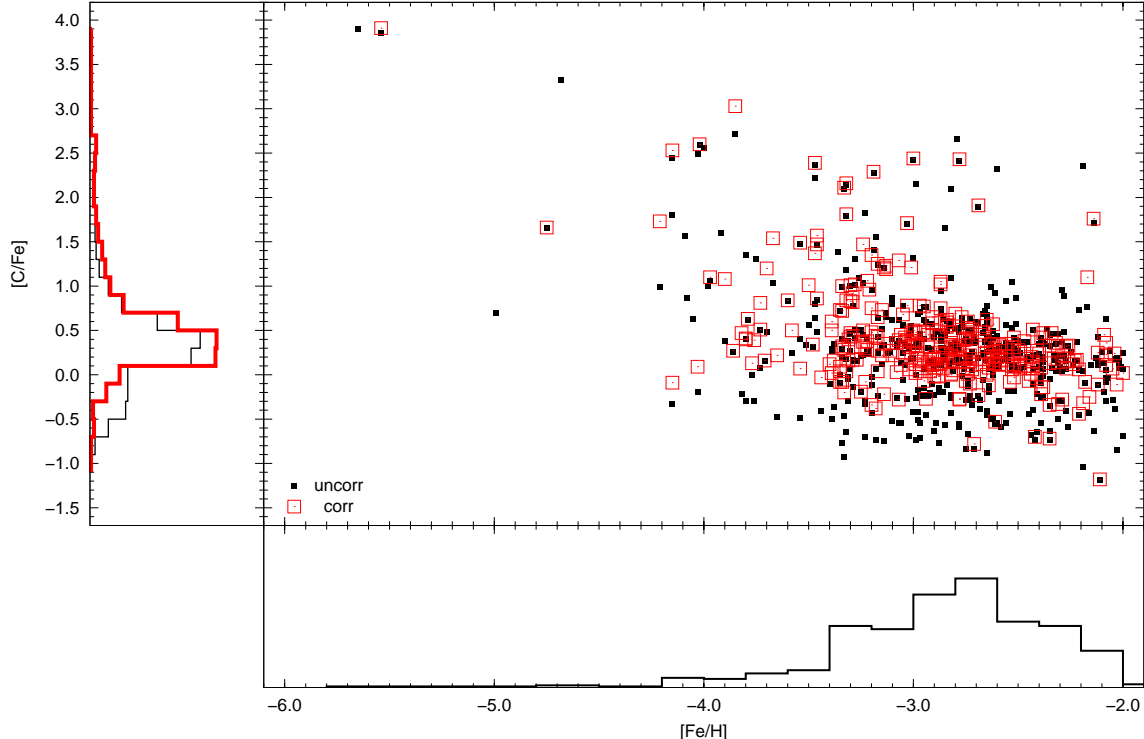


Figure 13. Carbonicities, $[C/Fe]$, for the literature stars, as a function of the metallicity, $[Fe/H]$, for the 505 stars with $[Fe/H] \leq -2.0$ selected from the literature. The black filled squares represent the measured abundances, while the red open squares show the corrected values for stars with non-zero corrections (for the $[N/Fe] = 0.00$ case). The marginal distributions of each variable, including the corrected values, are shown as histograms.

rection. In addition, the $\log g = 1.5$ case is where the corrections are mostly affected. Even then, the introduced shifts in $\log g$ do not produce deviations of more than ± 0.30 dex in the corrections. Once again, these are within the usual 2σ uncertainties related to observed $\log g$ and $[C/Fe]$ values.

5. CARBON-ABUNDANCE CORRECTIONS

5.1. Literature Sample

The correction procedure explained above was applied to the literature data described in Section 3. Figure 13 shows the distribution of the carbonicities for the 505 selected literature stars (with $[Fe/H] \leq -2.0$), as a function of metallicity, for both uncorrected (black filled dots) and corrected (red open circles) abundances. We only plot corrections different than zero. The applied corrections are based on the $[N/Fe] = 0.0$ model, and the histograms on the left and bottom panels also show the change in behavior of the carbon distribution. There is no significant change for stars with $[C/Fe] > +2.0$, and the distribution shifts to higher values for $[C/Fe] < +0.5$. The bulk of the stars in the $[C/Fe] < 0.0$ region have corrected values that place them in the $0.0 < [C/Fe] < +0.5$ range. This shift changes the overall behavior of the carbon abundances, and the applied corrections will affect the CEMP-star frequencies as a function of $[Fe/H]$ (see Section 6 for further details).

Figure 14 shows the distribution of the corrected $[C/Fe]$, as a function of luminosity (upper panel), and $\log g$ (lower panel), for the 505 stars selected from the literature. The evolutionary phases are based on the work of Gratton et al. (2000). The green solid line is

the CEMP criteria from Aoki et al. (2007), and the black solid lines are the theoretical models $[C/Fe] = -0.50/+0.70/+1.50/+2.50$ (assuming $[Fe/H] = -3.3$ and $[N/Fe] = 0.0$) shifted by 0.5 dex (see details on Section 4). Black filled squares are the measured abundances; red open squares show the corrected values (using the $[N/Fe] = 0.00$ corrections). Also shown (green solid line) is the luminosity-dependent CEMP criteria from Aoki et al. (2007). The models displayed in Figure 14 serve as guidelines, and were not used to correct all of the carbon abundances (see Section 4 for details).

One can see that the criteria set by Aoki et al. (2007) under-estimates the carbon depletion when compared to the shifted models, which leads to an under-estimation of the carbon-abundance corrections, and hence decreases the CEMP-star frequencies. The decreasing $[C/Fe]$ trend for increasing luminosities is flatter for the corrected values.

Assuming $[C/Fe] < +0.5$, the average carbon abundance for stars with $\log g < 2$ is $[C/Fe] = -0.21$ for the uncorrected abundances, and $[C/Fe] = +0.23$ for the corrected abundances, while for stars with $\log g > 3$ the average is $[C/Fe] = +0.24$. This agreement on the average carbon abundance also holds for $[C/Fe] < +0.7$ ($\log g < 2$: $[C/Fe] = -0.17$ uncorrected, $[C/Fe] = +0.27$ corrected, and $\log g > 3$: $[C/Fe] = +0.30$) and $[C/Fe] < +1.0$ ($\log g < 2$: $[C/Fe] = -0.13$ uncorrected, $[C/Fe] = +0.31$ corrected, and $\log g > 3$: $[C/Fe] = +0.35$). This demonstrates that our procedure is capable of recovering the amount of carbon depleted during the stellar evolution on the giant branch, and hence should yield more realistic values for the CEMP-star frequencies as a function of metallicity.

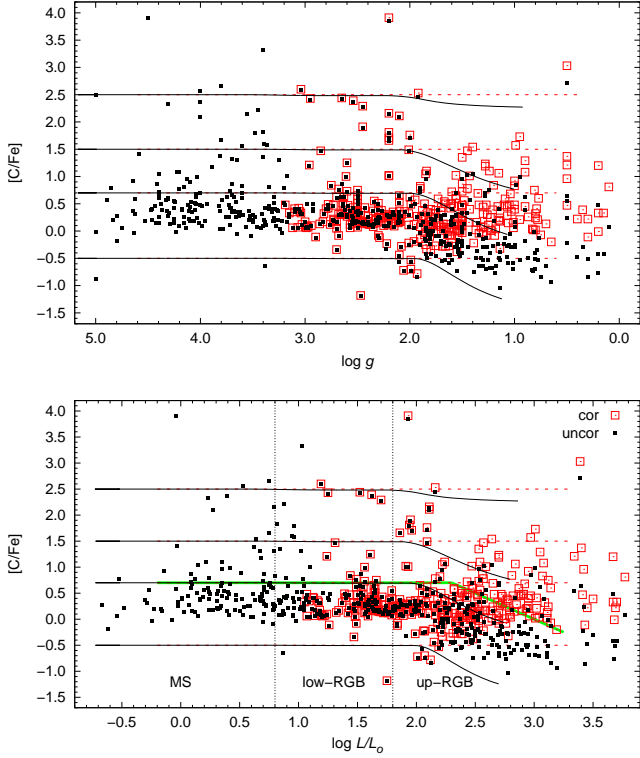


Figure 14. $[C/Fe]$, as a function of $\log g$ (upper panels) and luminosity (lower panel), for the 505 stars with $[Fe/H] \leq -2.0$ selected from the literature. The evolutionary phases are based on the work of Gratton et al. (2000). The green solid line is the CEMP criteria from Aoki et al. (2007). Black solid lines are the theoretical models for $[C/Fe] = -0.50/+0.70/+1.50/+2.50$ (assuming $[Fe/H] = -3.3$ and $[N/Fe] = 0.0$). The horizontal red dashed lines show the initial carbon abundances of the models. The black filled squares represent the measured abundances, while the red open squares show the corrected values for stars with non-zero corrections (for the $[N/Fe] = 0.00$ case).

5.2. The Gratton et al. Sample

We use the new theoretical models described in this work, and the corresponding carbon-abundance corrections, to further explore the data published by Gratton et al. (2000). These authors studied the mixing along the RGB in metal-poor field stars, and mapped out the effect on the observed $[C/Fe]$ and $[N/Fe]$. Figure 15 reproduces their Figure 10, where the upper panels show the behavior of $[C/Fe]$ and $[N/Fe]$, as a function of the $\log g$, and in the lower panels, as a function of the luminosity. The black filled squares are their published abundances, and the red open squares show the corrected carbon abundances, for case of $[N/Fe] = 0.0$. For comparison, we show the shifted theoretical models for $[N/Fe] = -0.50/-0.25/0.00$ (assuming $[Fe/H] = -1.3$ and $[C/Fe] = 0.0$) and $[C/Fe] = -0.50/-0.25/0.00$ (assuming $[Fe/H] = -1.3$ and $[N/Fe] = 0.0$). The $[C/Fe] = -0.25$ models are a linear interpolation between the 0.0 and -0.5 models.

It is remarkable how well the theoretical models shown in Figure 15 reproduce the behavior of both the carbon- and nitrogen-abundance ratios. Gratton et al. find that the average carbon-abundance ratio for their unevolved stars ($\log L/L_\odot < 0.8$) is $[C/Fe] = -0.09$, while the average for stars on the upper RGB is $[C/Fe] = -0.58$. By

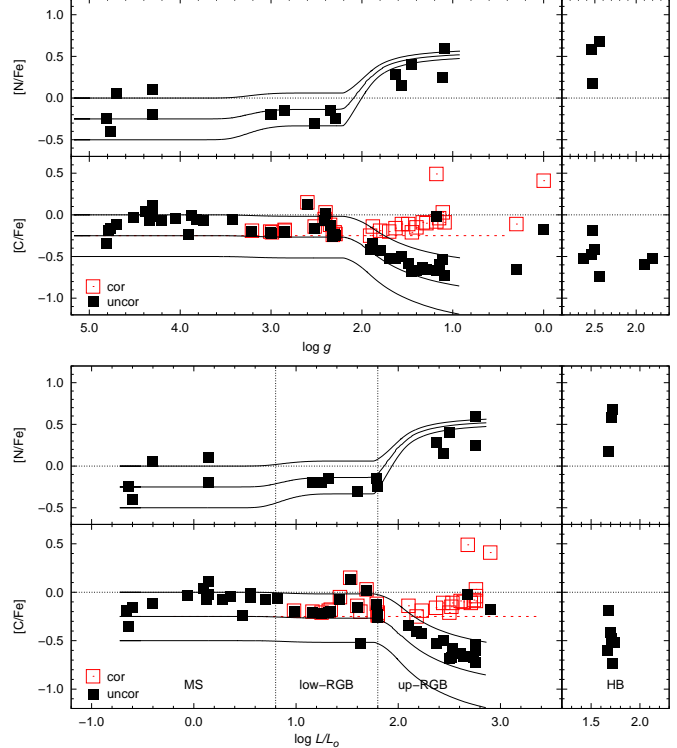


Figure 15. Carbon- and nitrogen-abundance ratios, as a function of $\log g$ (upper panels) and luminosity (lower panels), for the data from Gratton et al. (2000). The evolutionary phases were also taken from their Figure 7. Black solid lines are the theoretical models for $[N/Fe] = -0.50/-0.25/0.00$ (assuming $[Fe/H] = -1.3$ and $[C/Fe] = 0.0$) and $[C/Fe] = -0.50/-0.25/0.00$ (assuming $[Fe/H] = -1.3$ and $[N/Fe] = 0.0$). The horizontal red dashed lines show the initial carbon abundances of the models. The black filled squares represent the measured abundances, while the red open squares show the corrected values for stars with non-zero corrections (for the $[N/Fe] = 0.00$ case).

recalculating the average abundance for the upper-RGB stars using the corrected carbon abundances, we find an average of $[C/Fe] = -0.08$. The fact that the corrected average matches the one for unevolved stars may be a hint that our assumption of an early mixing onset compared to the models is correct, or further processing could have occurred in these objects.

6. THE CUMULATIVE FREQUENCIES OF CEMP STARS IN THE GALACTIC HALO AS A FUNCTION OF $[FE/H]$

Figure 16 shows the cumulative CEMP-star frequencies for metal-poor stars, for carbonicities $[C/Fe] \geq +0.5/+0.7/+1.0$, as a function metallicity ($-5.0 \leq [Fe/H] \leq -2.0$, see discussion in Section 1), for both uncorrected and corrected $[C/Fe]$. The $[Fe/H]$ step size is 0.1 dex, and the carbon corrections were taken considering initial $[N/Fe] = 0.0$ (see discussion in Section 4.3). The solid lines represent the frequencies for uncorrected abundances, the dashed lines are the frequencies for the corrected $[C/Fe]$, and the shaded areas highlight the differences between the distributions for a given $[C/Fe]$ range. Also shown on the plot are the cumulative CEMP-star frequencies of Frebel et al. (2006), Carollo et al. (2012), and Lee et al. (2013).

The cumulative CEMP frequencies for selected $[Fe/H]$ cuts are listed in Table 1. An important point to consider when comparing this new set of frequencies with previ-

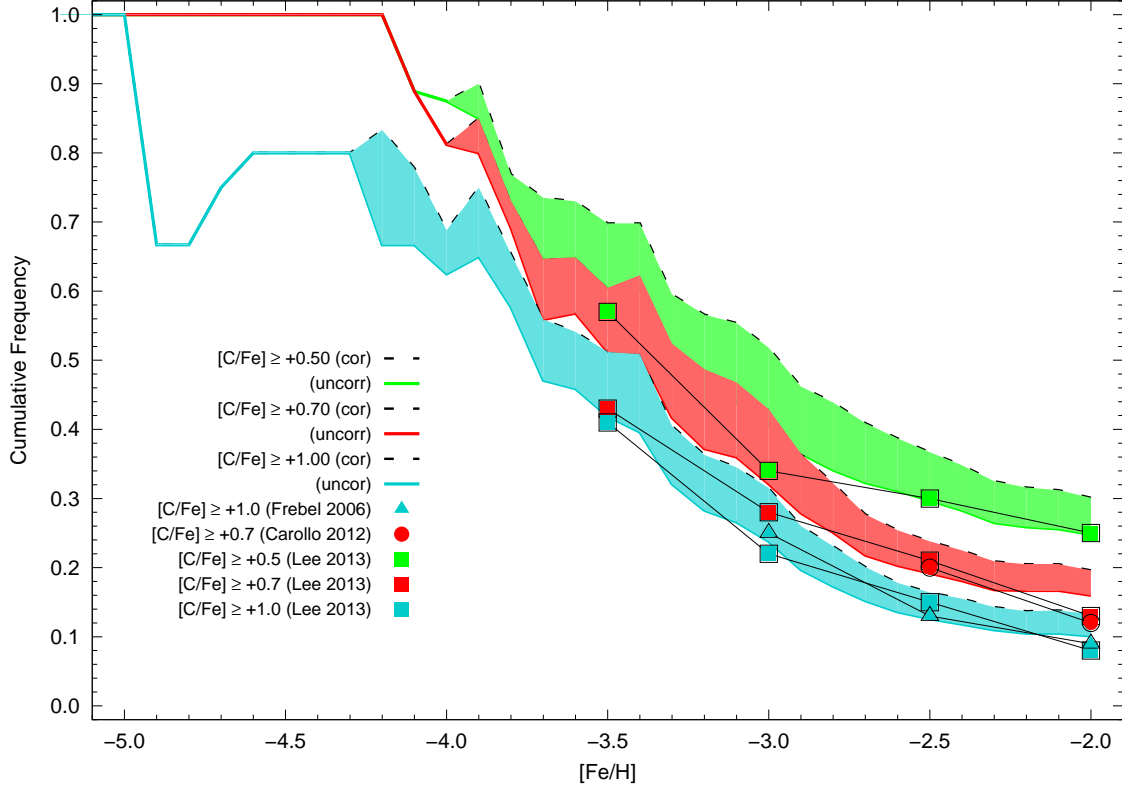


Figure 16. Cumulative frequencies of CEMP stars as a function of metallicity, based on the uncorrected (solid lines) and corrected (dashed lines) carbon abundances. The shaded areas highlight the differences in the frequencies for the corrected and uncorrected abundances. Note that, for the purpose of the corrections, $[N/Fe] = 0$ has been assumed. For comparison, we also show results from Frebel et al. (2006), Carollo et al. (2012), and Lee et al. (2013).

ous results is the fact that CEMP-*s* and CEMP-*r/s* stars were not specifically excluded previously, as they were based on medium-resolution ($R \sim 2,000$) spectroscopy, as opposed to this work, which uses data derived from high-resolution spectroscopy only. Since the metallicities for these stars are mostly concentrated in the $[\text{Fe}/\text{H}] > -3.0$ range, we expect over-estimated frequencies in this region. This effect can be quantified. The numbers in parenthesis in Table 1 show the difference (in %) between the frequencies calculated without any of the selection criteria presented in Section 3 and the adopted values shown in Table 1. As seen, the corrected cumulative CEMP frequencies for $[\text{Fe}/\text{H}] \leq -2.0$ and $[\text{C}/\text{Fe}] \geq +1.0$ roughly double (from 13% to $13\% + 14\% = 27\%$) if one takes into account the CEMP stars enriched via an *extrinsic* formation scenario. This effect is weaker for decreasing metallicities, and becomes negligible once the $[\text{Fe}/\text{H}] \leq -3.5$ range is reached. This is an anticipated result due to the absence of CEMP-*s* (and CEMP-*r/s*) stars at the lowest metallicities.

Inspection of Figure 16 and Table 1 reveals that, in most cases, the differences between the corrected and uncorrected values are within 10% of the entire sample; they reach up to 12% for $[\text{Fe}/\text{H}] \leq -3.0$ and $[\text{C}/\text{Fe}] \geq +0.50$ (40% uncorrected and 52% corrected), which represents a 30% increase. Our final derived cumulative CEMP-star frequencies for $[\text{C}/\text{Fe}] \geq +1.0$ (13% for $[\text{Fe}/\text{H}] \leq -2.0$, 32% for $[\text{Fe}/\text{H}] \leq -3.0$, 69% for $[\text{Fe}/\text{H}] \leq -4.0$, 100% for $[\text{Fe}/\text{H}] \leq -5.0$) are commensurate with the trend found by Frebel et al. (2006) for higher metallicities (9% for $[\text{Fe}/\text{H}] \leq -2.0$, and 25% for $[\text{Fe}/\text{H}] \leq -3.0$), even

though those determinations did not take into account the evolutionary stage, nor the addition of CEMP-*s* and CEMP-*r/s* to the analysis (and were based on a relatively small number of stars with measured $[\text{C}/\text{Fe}]$). We find that the cumulative CEMP-star frequencies estimated by Carollo et al. (2012) are slightly lower for $[\text{Fe}/\text{H}] \leq -2.0$, and agree well for $[\text{Fe}/\text{H}] \leq -2.5$. For Lee et al. (2013), the frequencies are overall lower for the $[\text{C}/\text{Fe}] \geq +0.5/+0.7$ bins, even when comparing with our uncorrected cumulative frequencies. For the $[\text{C}/\text{Fe}] \geq +1.0$ regime, the cumulative frequencies for stars with $[\text{Fe}/\text{H}] \leq -3.0$ agree well with the uncorrected frequencies from this work. Even though the sample sizes are considerably smaller than ours, we find that the cumulative CEMP-star frequencies (for stars with $[\text{C}/\text{Fe}] > +1.0$ and $[\text{Fe}/\text{H}] \leq -2.0$) from Lucatello et al. (2006) ($21\% \pm 2\%$) are over-estimated, while the results reported by Cohen et al. (2005) ($14\% \pm 4\%$) are lower by a few percent. Note that, even though these studies used high-resolution data for their frequency calculations, CEMP-*s* and CEMP-*r/s* were included.

There are no differences between the cumulative CEMP-star frequencies for the uncorrected and corrected cases for $[\text{Fe}/\text{H}] < -4.5$. Among the five stars analyzed in this metallicity range, there are two giants ($\log g = 2.2$), HE 0557–4840 and HE 0107–5240, with $[\text{C}/\text{Fe}]$ corrections of +0.01 dex and +0.06 dex, respectively. In addition, the most iron-poor star found to date, SMSS J031300.36–670839.3 ($[\text{Fe}/\text{H}] \leq -7.1$; Keller et al. 2014), has $\log g = 2.3$, and exhibits a remarkably high carbon abundance ($[\text{C}/\text{Fe}] > +4.5$), with negligible carbon

correction. The sudden decrease in the frequency between $-5.0 \geq [\text{Fe}/\text{H}] \geq -4.5$ and $[\text{C}/\text{Fe}] \geq +1.0$ is due to the presence of SDSS J102915 ($[\text{C}/\text{Fe}] \leq +0.7$; Caffau et al. 2011). It is important to note that this analysis is still limited by small-number statistics for stars in the $[\text{Fe}/\text{H}] \leq -4.0$ range, and further observations are required to firmly establish the frequencies.

To estimate the uncertainties on the derived frequencies from Table 1, we recalculated the corrected cumulative CEMP-star frequencies using nine different scenarios: (i) $[\text{N}/\text{Fe}] = -0.5$ model corrections; (ii) $[\text{N}/\text{Fe}] = +2.0$ model corrections; (iii) observed $\log g - 0.3$; (iv) observed $\log g + 0.3$; (v) observed $\log g$ adding a random uncertainty ranging from -0.3 dex to $+0.3$ dex; (vi) changing the CEMP-*s* and CEMP-*r/s* restriction to $[\text{Ba}/\text{Fe}] > +0.8$ (see Section 3 for further details); (vii) using carbon-abundance corrections determined by models only, without any shifts on $\log g$; (viii) introducing a $+0.3$ dex shift on the model $\log g$, and; (ix) taking into account 3D effects on the carbon abundances (Asplund 2005). The differences (in %) between the cumulative frequencies in each of these cases and the corrected values in Table 1 are shown in Table 2. Comparing the changes in the frequencies due to the choice of initial $[\text{N}/\text{Fe}]$ shows that these changes are always less than $\pm 1\%$. This is expected, since the largest differences in the corrections for $[\text{N}/\text{Fe}] = -0.5$ and $[\text{N}/\text{Fe}] = +2.0$ were from stars with measured $[\text{C}/\text{Fe}] < 0.0$. Concerning the changes in $\log g$, one can see that the differences are spread between -6% and $+8\%$ of the adopted values when all the stars are subject to the same shift in $\log g$. However, when adding a random uncertainty to the distribution, the absolute changes in the frequencies are less than $\pm 1\%$.

The changes in the CEMP-star frequencies for cases (vii) and (viii) are between $+1\%$ and -7% . This is within expectations, since the absence of or a $+0.3$ dex shift in $\log g$ under-estimate the carbon corrections for the stars in the upper RGB. We also considered the influence of possible 3D effects on the carbon-abundance determinations would have on our derived frequencies. It has been suggested (e.g., Collet et al. 2007) that these effects can lead to an over-estimate of $[\text{C}/\text{Fe}] = +0.5$ to $+0.9$ for the CH feature for red giants at $[\text{Fe}/\text{H}] \sim -3.0$. For the sample stars with $\log g \leq 3.0$, we applied $[\text{C}/\text{Fe}]$ offsets of -0.3 for $-2.5 < [\text{Fe}/\text{H}] \leq -2.0$, -0.5 for $-3.0 < [\text{Fe}/\text{H}] \leq -2.5$, and -0.7 for $[\text{Fe}/\text{H}] \leq -3.0$. The frequencies decreased between 5-14% for $[\text{Fe}/\text{H}] > -2.5$; the most affected cut was at $[\text{Fe}/\text{H}] \leq -3.5$, with a decrease ranging from 13-26%. The cumulative CEMP-star frequencies for stars with $[\text{Fe}/\text{H}] < -4.5$ were only affected for the case of $[\text{C}/\text{Fe}] \geq +1.0$. However, recent studies (Placco et al. 2014b) have found that the differences between carbon abundances determined from near-ultraviolet C I lines and the CH band at 4300Å are within ~ 0.2 dex for the $[\text{Fe}/\text{H}] = -3.8$ subgiant BD+44°493, so the 3D effect on the carbon abundance must be carefully evaluated.

7. CONCLUSIONS

CEMP-star frequencies are important inputs for Galactic chemical-evolution models (e.g., Kobayashi & Nakasato 2011), since they constrain the IMF in the early stages. In this work we present improved cumulative CEMP-star frequencies, taking into account the evolutionary status of metal-poor field stars. The amount of

carbon depleted during the evolution on the RGB was quantified by matching the observed carbon abundance to yields from stellar-evolution models. The offset added to the models to account for an early carbon depletion onset may indicate that the extent of thermohaline mixing is under-estimated, or that additional process(es), such as rotation, internal gravity waves, and magnetic fields (Maeder et al. 2013), must be considered.

Our final derived cumulative CEMP-star frequencies are: (i) $[\text{C}/\text{Fe}] \geq +0.7$ – 20% for $[\text{Fe}/\text{H}] \leq -2.0$, 43% for $[\text{Fe}/\text{H}] \leq -3.0$, 81% for $[\text{Fe}/\text{H}] \leq -4.0$, and 100% for $[\text{Fe}/\text{H}] \leq -5.0$; (ii) $[\text{C}/\text{Fe}] \geq +1.0$ – 13% for $[\text{Fe}/\text{H}] \leq -2.0$, 32% for $[\text{Fe}/\text{H}] \leq -3.0$, 69% for $[\text{Fe}/\text{H}] \leq -4.0$, and 100% for $[\text{Fe}/\text{H}] \leq -5.0$. For this exercise we used 505 stars with $[\text{Fe}/\text{H}] \leq -2.0$ from the literature, with atmospheric parameters and abundances determined from high-resolution spectroscopy.

This is the largest high-resolution sample yet considered for such an analysis. These values exclude the recognized CEMP-*s* and CEMP-*r/s* stars from the calculations, since their observed carbon abundance is “contaminated” from its evolved AGB companion in a binary system. We also developed an online tool that provides the carbon corrections for a given set of $\log g$, $[\text{Fe}/\text{H}]$, and $[\text{C}/\text{Fe}]$. Further work may include correction of carbon abundances for stars observed with medium-resolution spectroscopy (Frebel et al. 2006; Placco et al. 2010, 2011; Carollo et al. 2012; Lee et al. 2013; Kordopatis et al. 2013; Beers et al. 2014). However, reliable $\log g$ information must be provided, to avoid large uncertainties on the carbon abundance corrections.

Table 3 lists the input data used for the determination of the CEMP-star frequencies, as well as the correction for the $[\text{N}/\text{Fe}] = 0.0$ case. Also listed, for completeness, are the CEMP-*s* and CEMP-*r/s* stars excluded from the calculations. Even though these stars are not suitable for the CEMP-star frequency determinations, they also experience carbon depletion during their evolution, and our machinery allows its measurement. The luminosities are derived from the Aoki et al. (2007) prescription, using $M = 0.8 M_{\odot}$. It is interesting to note from Table 3 that 16 stars are CEMP stars (based on corrected $[\text{C}/\text{Fe}] \geq +0.7$), but are not sub-classified further, due to lack of information on their $[\text{Ba}/\text{Fe}]$ ratios. Of these, 11 stars have $[\text{Fe}/\text{H}] < -3.0$, which is the range where CEMP-no stars are most common. In addition, there are 53 stars which can be considered carbon-enriched, with $+0.5 \leq [\text{C}/\text{Fe}] \leq +0.7$, but that do not satisfy our criterion for classification as CEMP stars. Of these, 46 have measured $[\text{Ba}/\text{Fe}]$, with 41 exhibiting $[\text{Ba}/\text{Fe}] < 0.0$. These can be classified as likely CEMP-no stars, and further observations of such stars should help resolve their proper classifications.

Even though the cumulative frequencies presented in this work only changed by modest amounts when compared to the uncorrected results, our approach of taking into account the evolutionary status of the stars and also excluding CEMP-*s* and CEMP-*r/s* stars from the estimates provides the currently most reliable estimate of the CEMP frequencies. This effort would clearly benefit from additional $[\text{N}/\text{Fe}]$ measurements for a large number of stars in our sample, as well as measurements for $[\text{Ba}/\text{Fe}]$ (and $[\text{Eu}/\text{Fe}]$) in order to enable the identification of additional CEMP-no stars. As additional obser-

vations of evolved CEMP stars near the tip of the RGB become available, the impact of our corrections on the derived cumulative CEMP-star frequencies will increase.

Furthermore, the ability to describe the true CEMP-star frequencies allows the quantification and assessment of the proper formation channels of the two distinctive metal-poor stellar populations in the Galactic halo at $[Fe/H] < -3.0$: carbon-normal and carbon-rich (Norris et al. 2013b). These two populations are thought to be formed by gas clouds that were influenced by at least two different primary cooling channels (Frebel et al. 2007; Schneider et al. 2012; Ji et al. 2014). Once the number and type of progenitors are quantified, it will be possible to build a more reliable model of the stellar populations of the early Milky Way, and by extension, for other galaxies. Besides that, by having a more reliable characterization of these populations, it will become possible to compare the occurrence rate of CEMP-no stars with the recently discovered carbon-enhanced damped Ly α systems (Cooke et al. 2011, 2012) which carry abundance patterns that resemble those from massive, carbon-producing first stars.

V.M.P. is a Gemini Science Fellow, and acknowledges support from the Gemini Observatory. A.F. is supported by NSF CAREER grant AST-1255160. T.C.B. acknowledges partial support for this work from grants PHY 08-22648; Physics Frontier Center/Joint Institute or Nuclear Astrophysics (JINA), and PHY 14-30152; Physics Frontier Center/JINA Center for the Evolution of the Elements (JINA-CEE), awarded by the US National Science Foundation. R.J.S. is the recipient of a Sofja Kovalevskaja Award from the Alexander von Humboldt Foundation.

REFERENCES

- Akerman, C. J., Carigi, L., Nissen, P. E., Pettini, M., & Asplund, M. 2004, A&A, 414, 931
- Allen, D. M., Ryan, S. G., Rossi, S., Beers, T. C., & Tsangarides, S. A. 2012, A&A, 548, A34
- Angelou, G. C., Church, R. P., Stancliffe, R. J., Lattanzio, J. C., & Smith, G. H. 2011, ApJ, 728, 79
- Angelou, G. C., Stancliffe, R. J., Church, R. P., Lattanzio, J. C., & Smith, G. H. 2012, ApJ, 749, 128
- Aoki, W., Beers, T. C., Christlieb, N., et al. 2007, ApJ, 655, 492
- Aoki, W., Norris, J. E., Ryan, S. G., Beers, T. C., & Ando, H. 2002, PASJ, 54, 933
- Aoki, W., Suda, T., Boyd, R. N., Kajino, T., & Famiano, M. A. 2013, ApJ, 766, L13
- Aoki, W., Honda, S., Beers, T. C., et al. 2005, ApJ, 632, 611
- Aoki, W., Frebel, A., Christlieb, N., et al. 2006, ApJ, 639, 897
- Aoki, W., Beers, T. C., Sivarani, T., et al. 2008, ApJ, 678, 1351
- Asplund, M. 2005, ARA&A, 43, 481
- Asplund, M., Grevesse, N., Sauval, A. J., & Scott, P. 2009, ARA&A, 47, 481
- Barklem, P. S., Christlieb, N., Beers, T. C., et al. 2005, A&A, 439, 129
- Beers, T. C., & Christlieb, N. 2005, ARA&A, 43, 531
- Beers, T. C., Norris, J. E., Placco, V. M., et al. 2014, ApJ, 794, 58
- Bisterzo, S., Gallino, R., Straniero, O., Cristallo, S., & Käppeler, F. 2011, MNRAS, 418, 284
- Caffau, E., Bonifacio, P., François, P., et al. 2011, Nature, 477, 67
- Carollo, D., Freeman, K., Beers, T. C., et al. 2014, ApJ, 788, 180
- Carollo, D., Beers, T. C., Bovy, J., et al. 2012, ApJ, 744, 195
- Charbonnel, C., & Zahn, J.-P. 2007, A&A, 467, L15
- Christlieb, N., Bessell, M. S., Beers, T. C., et al. 2002, Nature, 419, 904
- Christlieb, N., Beers, T. C., Barklem, P. S., et al. 2004, A&A, 428, 1027
- Cohen, J. G., Christlieb, N., McWilliam, A., et al. 2008, ApJ, 672, 320
- Cohen, J. G., Christlieb, N., Thompson, I., et al. 2013, ApJ, 778, 56
- Cohen, J. G., Shectman, S., Thompson, I., et al. 2005, ApJ, 633, L109
- Collet, R., Asplund, M., & Trampedach, R. 2007, A&A, 469, 687
- Cooke, R., Pettini, M., & Murphy, M. T. 2012, MNRAS, 3437
- Cooke, R., Pettini, M., Steidel, C. C., Rudie, G. C., & Nissen, P. E. 2011, MNRAS, 417, 1534
- Cooke, R. J., & Madau, P. 2014, ApJ, 791, 116
- Cui, W. Y., Sivarani, T., & Christlieb, N. 2013, A&A, 558, A36
- Demarque, P., Woo, J.-H., Kim, Y.-C., & Yi, S. K. 2004, ApJS, 155, 667
- Denissenkov, P. A., & Merryfield, W. J. 2011, ApJ, 727, L8
- Eggleton, P. P. 1971, MNRAS, 151, 351
- Frebel, A., Johnson, J. L., & Bromm, V. 2007, MNRAS, 380, L40
- Frebel, A., Kirby, E. N., & Simon, J. D. 2010, Nature, 464, 72
- Frebel, A., & Norris, J. E. 2013, Metal-Poor Stars and the Chemical Enrichment of the Universe (Published), 55
- Frebel, A., Aoki, W., Christlieb, N., et al. 2005, Nature, 434, 871
- Frebel, A., Christlieb, N., Norris, J. E., et al. 2006, ApJ, 652, 1585
- Goswami, A., Aoki, W., Beers, T. C., et al. 2006, MNRAS, 372, 343
- Gratton, R. G., Sneden, C., Carretta, E., & Bragaglia, A. 2000, A&A, 354, 169
- Hansen, T., Andersen, J., Nordström, B., Buchhave, L. A., & Beers, T. C. 2011, ApJ, 743, L1
- Hansen, T., Hansen, C. J., Christlieb, N., et al. 2014, ApJ, 787, 162
- Herwig, F. 2005, ARA&A, 43, 435
- Hollek, J. K., Frebel, A., Placco, V. M., et al. 2014, ApJ submitted
- Hollek, J. K., Frebel, A., Roederer, I. U., et al. 2011, ApJ, 742, 54
- Ito, H., Aoki, W., Beers, T. C., et al. 2013, ApJ, 773, 33
- Ito, H., Aoki, W., Honda, S., & Beers, T. C. 2009, ApJ, 698, L37
- Ji, A. P., Frebel, A., & Bromm, V. 2014, ApJ, 782, 95
- Johnson, J. A., Herwig, F., Beers, T. C., & Christlieb, N. 2007, ApJ, 658, 1203
- Jonsell, K., Barklem, P. S., Gustafsson, B., et al. 2006, A&A, 451, 651
- Keller, S. C., Bessell, M. S., Frebel, A., et al. 2014, Nature, 506, 463
- Kippenhahn, R., Ruschenplatt, G., & Thomas, H.-C. 1980, A&A, 91, 175
- Kobayashi, C., & Nakasato, N. 2011, ApJ, 729, 16
- Kordopatis, G., Gilmore, G., Steinmetz, M., et al. 2013, AJ, 146, 134
- Lai, D. K., Bolte, M., Johnson, J. A., et al. 2008, ApJ, 681, 1524
- Lai, D. K., Johnson, J. A., Bolte, M., & Lucatello, S. 2007, ApJ, 667, 1185
- Lee, Y. S., Suda, T., Beers, T. C., & Stancliffe, R. J. 2014, ApJ, 788, 131
- Lee, Y. S., Beers, T. C., Masseron, T., et al. 2013, AJ, 146, 132
- Lucatello, S., Beers, T. C., Christlieb, N., et al. 2006, ApJ, 652, L37
- Lucatello, S., Tsangarides, S., Beers, T. C., et al. 2005, ApJ, 625, 825
- Maeder, A., Meynet, G., Lagarde, N., & Charbonnel, C. 2013, A&A, 553, A1
- Mashonkina, L., Ryabtsev, A., & Frebel, A. 2012, A&A, 540, A98
- Masseron, T., Johnson, J. A., Lucatello, S., et al. 2012, ApJ, 751, 14
- Masseron, T., Johnson, J. A., Plez, B., et al. 2010, A&A, 509, A93+
- Mathis, S., Decressin, T., Eggenberger, P., & Charbonnel, C. 2013, A&A, 558, A11
- McWilliam, A., Preston, G. W., Sneden, C., & Searle, L. 1995, AJ, 109, 2757
- Meléndez, J., & Barbuy, B. 2002, ApJ, 575, 474
- Meynet, G., Ekström, S., & Maeder, A. 2006, A&A, 447, 623
- Meynet, G., Hirschi, R., Ekstrom, S., et al. 2010, A&A, 521, A30
- Nomoto, K., Tominaga, N., Umeda, H., Kobayashi, C., & Maeda, K. 2006, Nuclear Physics A, 777, 424
- Norris, J. E., Christlieb, N., Korn, A. J., et al. 2007, ApJ, 670, 774

- Norris, J. E., Bessell, M. S., Yong, D., et al. 2013a, *ApJ*, 762, 25
 Norris, J. E., Yong, D., Bessell, M. S., et al. 2013b, *ApJ*, 762, 28
 Placco, V. M., Frebel, A., Beers, T. C., et al. 2014a, *ApJ*, 781, 40
 —. 2013, *ApJ*, 770, 104
 Placco, V. M., Kennedy, C. R., Rossi, S., et al. 2010, *AJ*, 139, 1051
 Placco, V. M., Kennedy, C. R., Beers, T. C., et al. 2011, *AJ*, 142, 188
 Placco, V. M., Beers, T. C., Roederer, I. U., et al. 2014b, *ApJ*, 790, 34
 Pols, O. R., Izzard, R. G., Stancliffe, R. J., & Glebbeek, E. 2012, *A&A*, 547, A76
 Preston, G. W., & Sneden, C. 2001, *AJ*, 122, 1545
 Preston, G. W., Sneden, C., Thompson, I. B., Shectman, S. A., & Burley, G. S. 2006, *AJ*, 132, 85
 Roederer, I. U., Lawler, J. E., Sneden, C., et al. 2008a, *ApJ*, 675, 723
 Roederer, I. U., Preston, G. W., Thompson, I. B., Shectman, S. A., & Sneden, C. 2014, *ApJ*, 784, 158
 Roederer, I. U., Sneden, C., Thompson, I. B., Preston, G. W., & Shectman, S. A. 2010, *ApJ*, 711, 573
 Roederer, I. U., Frebel, A., Shetrone, M. D., et al. 2008b, *ApJ*, 679, 1549
 Schneider, R., Omukai, K., Bianchi, S., & Valiante, R. 2012, *MNRAS*, 419, 1566
 Simmerer, J., Sneden, C., Cowan, J. J., et al. 2004, *ApJ*, 617, 1091
 Sivarani, T., Beers, T. C., Bonifacio, P., et al. 2006, *A&A*, 459, 125
 Sneden, C., Cowan, J. J., Lawler, J. E., et al. 2003, *ApJ*, 591, 936
 Spite, M., Caffau, E., Bonifacio, P., et al. 2013, *A&A*, 552, A107
 Spite, M., Cayrel, R., Hill, V., et al. 2006, *A&A*, 455, 291
 Stancliffe, R. J., Church, R. P., Angelou, G. C., & Lattanzio, J. C. 2009, *MNRAS*, 396, 2313
 Stancliffe, R. J., & Eldridge, J. J. 2009, *MNRAS*, 396, 1699
 Stancliffe, R. J., & Lattanzio, J. C. 2011, Why Galaxies Care about AGB Stars II: Shining Examples and Common Inhabitants, 445, 29
 Suda, T., Katsuta, Y., Yamada, S., et al. 2008, *PASJ*, 60, 1159
 Thompson, I. B., Ivans, I. I., Bisterzo, S., et al. 2008, *ApJ*, 677, 556
 Tominaga, N., Umeda, H., & Nomoto, K. 2007, *ApJ*, 660, 516
 Ulrich, R. K. 1972, *ApJ*, 172, 165
 Umeda, H., & Nomoto, K. 2005, *ApJ*, 619, 427
 Viallet, M., Meakin, C., Arnett, D., & Mocák, M. 2013, *ApJ*, 769, 1
 Woosley, S. E., & Weaver, T. A. 1995, *ApJS*, 101, 181
 Yong, D., Norris, J. E., Bessell, M. S., et al. 2013, *ApJ*, 762, 26
 Zhang, L., Karlsson, T., Christlieb, N., et al. 2011, *A&A*, 528, A92

Table 1
Cumulative CEMP-star Frequencies

[Fe/H]≤	% [C/Fe] (+ΔCEMP- <i>s/-rs</i>)					
	≥ +0.50		≥ +0.70		≥ +1.00	
	uncor	cor	uncor	cor	uncor	cor
-2.0	25 (+12)	30 (+12)	16 (+14)	20 (+13)	10 (+14)	13 (+14)
-2.5	30 (+09)	37 (+08)	19 (+11)	24 (+10)	13 (+11)	16 (+12)
-3.0	40 (+07)	52 (+05)	32 (+07)	43 (+05)	24 (+07)	32 (+06)
-3.5	60 (+00)	70 (+00)	51 (+00)	60 (+00)	42 (+00)	51 (+00)
-4.0	88 (+00)	88 (+00)	81 (+00)	81 (+00)	62 (+00)	69 (+00)
-4.5	100 (+00)	100 (+00)	100 (+00)	100 (+00)	80 (+00)	80 (+00)
-5.0	100 (+00)	100 (+00)	100 (+00)	100 (+00)	100 (+00)	100 (+00)

Note. — The values in parenthesis show the increase (in %) in the cumulative CEMP-star frequencies due to the addition of CEMP-*s* and CEMP-*r/s* stars.

Table 2
Uncertainties in Derived Cumulative CEMP-star Frequencies

[Fe/H]≤	(i) [N/Fe] -0.5	(ii) [N/Fe] +2.0	(iii) $\Delta \log g$ +0.3	(iv) $\Delta \log g$ -0.3	(v) $\Delta \log g$ random	(vi) [Ba/Fe] < +0.8	(vii) Model only	(viii) Model +0.3	(ix) $\Delta [C/Fe]$ 3D
$\Delta\%$ ([C/Fe] ≥ +0.50)									
-2.0	1	0	-3	-2	1	0	-1	1	-10
-2.5	0	0	-4	-2	0	1	-4	-2	-14
-3.0	1	0	-6	-4	0	0	-7	-3	-20
-3.5	0	0	-3	0	0	0	-3	-3	-26
-4.0	0	0	0	0	0	0	0	0	-13
-4.5	0	0	0	0	0	0	0	0	0
-5.0	0	0	0	0	0	0	0	0	0
$\Delta\%$ ([C/Fe] ≥ +0.70)									
-2.0	0	0	-1	5	-1	0	-1	0	-7
-2.5	0	0	-1	6	0	1	-3	-2	-9
-3.0	0	0	-2	8	-1	1	-7	-4	-18
-3.5	0	0	-2	0	0	0	-4	-2	-16
-4.0	0	0	0	0	0	0	0	0	-6
-4.5	0	0	0	0	0	0	0	0	0
-5.0	0	0	0	0	0	0	0	0	0
$\Delta\%$ ([C/Fe] ≥ +1.00)									
-2.0	-1	0	4	1	0	1	0	1	-5
-2.5	0	0	5	1	0	0	-2	0	-6
-3.0	-1	0	6	1	0	0	-5	-2	-14
-3.5	0	0	3	0	0	0	-4	-2	-18
-4.0	0	0	0	0	0	0	0	0	-13
-4.5	0	0	0	0	0	0	0	0	-20
-5.0	0	0	0	0	0	0	0	0	0

Table 3
Data for Literature Stars

Name	T_{eff} (K)	$\log g$ (cgs)	$\log L$ (L_{\odot})	[Fe/H]	[N/Fe]	[C/Fe]	$\Delta[\text{C}/\text{Fe}]$ ([N/Fe]=0)	$[\text{C}/\text{Fe}]_c$	[Sr/Fe]	[Ba/Fe]	Class	I/O	Ref.	
BD+02:3375	5926	4.63	-0.24	-2.08	...	-0.04	0.00	-0.04	1		Lai et al. (2007)	
BD+03:740	6485	4.31	0.23	-2.70	$\leq +0.29$	+0.59	0.00	+0.59	...	-0.42	1		Yong et al. (2013)	
BD+06:0648	4400	0.90	2.97	-2.09	...	-0.19	+0.64	+0.45	1		Aoki et al. (2008)	
BD+10:2495	4710	1.30	2.69	-2.31	...	-0.30	+0.62	+0.32	1		Roederer et al. (2010)	
BD+17:3248	5240	2.72	1.45	-2.17	+0.65	-0.37	+0.01	-0.36	...	+0.69	0		Yong et al. (2013)	
BD+23:3130	5262	2.76	1.42	-2.52	-0.54	+0.11	+0.01	+0.12	...	-0.56	1		Yong et al. (2013)	
BD+24:1676	6241	3.81	0.67	-2.46	$\leq +0.21$	+0.37	0.00	+0.37	-0.05	-0.33	1		Lai et al. (2008)	
BD+44:493	5430	3.40	0.84	-3.80	+0.32	+1.35	0.00	+1.35	...	-0.60	CEMP-no	1		Ito et al. (2013)
BD-01:2582	5148	2.86	1.28	-2.21	...	+0.76	+0.01	+0.77	...	+1.50	CEMP-s/rs	0		Simmerer et al. (2004)
BD-04:3208	6360	4.01	0.50	-2.27	...	+0.15	0.00	+0.15	1		Akerman et al. (2004)	
BD-18:0271	4245	0.70	3.11	-2.35	...	-0.64	+0.77	+0.13	1		Meléndez & Barbuy (2002)	
BD-18:5550	4558	0.81	3.12	-3.20	-0.36	-0.02	+0.77	+0.75	...	-0.74	CEMP-no	1		Yong et al. (2013)
BS 16023-046	6571	4.25	0.32	-2.83	...	+0.55	0.00	+0.55	-0.08	...	1		Yong et al. (2013)	
BS 16033-008	5300	2.70	1.49	-2.84	...	+0.61	+0.01	+0.62	-0.31	-1.20	1		Aoki et al. (2005)	
BS 16076-006	5566	3.32	0.96	-3.51	...	+0.34	0.00	+0.34	$\leq +0.10$	≤ -1.00	1		Yong et al. (2013)	
BS 16077-007	6486	4.31	0.23	-2.77	$\leq +0.80$	+0.60	0.00	+0.60	+0.21	-0.23	1		Yong et al. (2013)	
BS 16080-054	4902	1.75	2.31	-2.94	+0.75	-0.45	+0.18	-0.27	+0.38	-0.21	1		Yong et al. (2013)	
BS 16082-129	4868	1.67	2.38	-2.84	...	+0.29	+0.25	+0.54	-0.69	-0.97	1		Yong et al. (2013)	
BS 16083-172	5300	3.10	1.09	-2.53	...	+0.34	+0.01	+0.35	+0.19	-0.33	1		Aoki et al. (2005)	
BS 16084-160	4727	1.27	2.72	-3.20	+0.78	-0.12	+0.60	+0.48	-2.07	-2.06	1		Yong et al. (2013)	
BS 16085-050	4882	1.93	2.12	-2.71	...	-0.84	+0.06	-0.78	-1.67	-1.62	1		Yong et al. (2013)	
BS 16089-013	4900	1.70	2.36	-2.82	...	-0.23	+0.24	+0.01	+0.21	-0.09	1		Aoki et al. (2005)	
BS 16467-062	5310	2.80	1.40	-3.80	$\leq +0.45$	+0.40	+0.01	+0.41	-1.67	≤ -0.57	1		Yong et al. (2013)	
BS 16469-075	4919	1.78	2.28	-3.25	...	+0.21	+0.11	+0.32	+0.27	-1.12	1		Yong et al. (2013)	
BS 16472-018	4946	2.08	1.99	-2.29	...	-0.29	+0.01	-0.28	+0.19	-0.14	1		Lai et al. (2007)	
BS 16477-003	4879	1.66	2.39	-3.39	≤ -0.26	+0.29	+0.21	+0.50	+0.11	-0.45	1		Yong et al. (2013)	
BS 16543-092	4523	1.14	2.78	-2.19	...	-1.04	+0.72	-0.32	-0.36	-0.63	1		Lai et al. (2007)	
BS 16543-097	5000	2.10	1.99	-2.52	...	+0.29	+0.02	+0.31	+0.12	-0.12	1		Aoki et al. (2005)	
BS 16547-006	6047	3.72	0.70	-2.21	...	+0.73	0.00	+0.73	-0.44	-0.52	CEMP-no	1		Lai et al. (2007)
BS 16550-087	4754	1.32	2.68	-3.54	+1.11	-0.49	+0.56	+0.07	+0.53	-0.75	1		Yong et al. (2013)	
BS 16928-053	4679	1.16	2.82	-2.93	+1.05	-0.24	+0.69	+0.45	-0.19	-0.79	1		Yong et al. (2013)	
BS 16929-005	5229	2.61	1.56	-3.34	+0.32	+0.99	+0.01	+1.00	...	-0.41	CEMP-no	1		Yong et al. (2013)
BS 16934-002	4500	1.00	2.91	-2.82	+0.64	-0.26	+0.74	+0.48	-1.27	-1.65	1		Aoki et al. (2007)	
BS 16945-054	5281	2.99	1.20	-2.76	...	+0.06	+0.01	+0.07	-0.04	-0.01	1		Lai et al. (2007)	
BS 16968-061	6343	3.82	0.69	-2.85	...	+0.45	0.00	+0.45	-0.47	-0.23	1		Yong et al. (2013)	
BS 16981-009	5259	2.92	1.26	-2.71	...	+0.36	0.00	+0.36	1		Lai et al. (2007)	
BS 17139-007	5918	3.66	0.72	-2.25	...	+0.26	0.00	+0.26	-0.55	-0.62	1		Lai et al. (2007)	
BS 17439-065	5100	1.60	2.53	-2.39	...	-0.54	+0.40	-0.14	-0.22	-0.42	1		Aoki et al. (2005)	
BS 17569-049	4645	1.09	2.87	-2.84	+0.86	-0.12	+0.71	+0.59	+0.38	+0.20	1		Yong et al. (2013)	
BS 17570-063	6233	4.46	0.01	-2.95	...	+0.40	0.00	+0.40	+0.08	-0.26	1		Yong et al. (2013)	
BS 17583-100	5950	3.66	0.73	-2.53	...	+0.53	0.00	+0.53	+0.20	-0.33	1		Yong et al. (2013)	
CD-35:14849	6125	4.11	0.33	-2.41	...	+0.22	0.00	+0.22	1		Akerman et al. (2004)	
CD-38:245	4857	1.54	2.50	-4.15	+1.07	-0.33	+0.24	-0.09	...	-0.76	1		Yong et al. (2013)	
CD-42:14278	5812	4.25	0.10	-2.12	...	+0.15	0.00	+0.15	1		Akerman et al. (2004)	
CS 22166-016	5388	3.26	0.96	-2.30	...	+0.21	0.00	+0.21	+0.30	-0.24	1		Lai et al. (2007)	
CS 22169-035	4654	1.10	2.87	-2.95	+1.02	-0.24	+0.72	+0.48	+0.02	-1.19	1		Yong et al. (2013)	
CS 22172-002	4893	1.68	2.37	-3.77	+0.24	0.00	+0.13	+0.13	-1.21	-1.17	1		Yong et al. (2013)	
CS 22174-007	5265	2.78	1.40	-2.39	$\leq +1.42$	+0.41	+0.01	+0.42	...	-0.14	1		Yong et al. (2013)	
CS 22174-012	4934	2.06	2.01	-2.35	...	-0.74	+0.02	-0.72	-0.45	-0.95	1		Lai et al. (2007)	
CS 22175-007	5108	2.46	1.67	-2.81	...	+0.15	+0.01	+0.16	+0.27	-0.52	1		Barklem et al. (2005)	
CS 22177-009	6423	4.37	0.16	-2.98	...	+0.38	0.00	+0.38	-0.26	...	1		Yong et al. (2013)	
CS 22182-033	5700	3.30	1.02	-2.67	...	+0.24	0.00	+0.24	+0.01	-0.41	1		Preston et al. (2006)	
CS 22183-015	5450	3.00	1.24	-2.82	+2.09	+2.33	+0.02	+2.35	...	+1.85	CEMP-s/rs	0		Masseron et al. (2012)
CS 22183-031	5202	2.54	1.62	-3.17	...	+0.42	+0.01	+0.43	+0.14	-0.33	1		Yong et al. (2013)	

Table 3 — *Continued*

Name	T_{eff} (K)	$\log g$ (cgs)	$\log L$ (L_{\odot})	[Fe/H]	[N/Fe]	[C/Fe]	$\Delta[\text{C}/\text{Fe}]$ ([N/Fe]=0)	$[\text{C}/\text{Fe}]_c$	[Sr/Fe]	[Ba/Fe]	Class	I/O	Ref.	
CS 22185–007	5193	2.73	1.43	−2.28	...	+0.21	+0.01	+0.22	−0.42	−0.51	1		Lai et al. (2007)	
CS 22186–023	5066	2.19	1.92	−2.72	...	+0.26	+0.01	+0.27	−0.05	−0.98	1		Barklem et al. (2005)	
CS 22186–025	4871	1.66	2.39	−3.07	+0.98	−0.54	+0.26	−0.28	−0.02	+0.02	1		Yong et al. (2013)	
CS 22189–009	4944	1.83	2.24	−3.48	+0.27	+0.31	+0.03	+0.34	−0.85	−1.29	1		Yong et al. (2013)	
CS 22872–102	5911	3.60	0.78	−2.94	\leq +0.55	+0.60	0.00	+0.60	−0.17	−0.62	1		Yong et al. (2013)	
CS 22873–055	4551	0.82	3.11	−2.99	+1.07	−0.73	+0.75	+0.02	−0.39	−0.45	1		Yong et al. (2013)	
CS 22873–128	4960	2.10	1.98	−2.86	...	+0.18	+0.01	+0.19	−0.43	−0.96	1		McWilliam et al. (1995)	
CS 22873–166	4516	0.77	3.14	−2.74	+1.05	−0.13	+0.73	+0.60	+0.18	−0.70	1		Yong et al. (2013)	
CS 22877–001	4790	1.45	2.57	−3.24	−0.15	+1.03	+0.44	+1.47	−0.02	−0.58	CEMP-no	1		Roederer et al. (2014)
CS 22877–011	5130	2.35	1.79	−2.90	...	+0.07	+0.01	+0.08	−1.21	−1.34	1		McWilliam et al. (1995)	
CS 22878–027	6319	4.41	0.09	−2.51	\leq +1.06	+0.86	0.00	+0.86	−0.29	\leq −0.75	CEMP-no	1		Yong et al. (2013)
CS 22878–101	4796	1.44	2.58	−3.31	+1.33	−0.29	+0.45	+0.16	−0.13	−0.64	1		Yong et al. (2013)	
CS 22878–121	5450	1.90	2.34	−2.38	...	−0.25	+0.11	−0.14	+0.18	−0.08	1		Preston et al. (2006)	
CS 22879–097	5800	2.30	2.05	−2.43	...	+0.50	+0.01	+0.51	+0.26	−0.47	1		Preston et al. (2006)	
CS 22879–103	5775	1.85	2.49	−2.08	...	+0.05	+0.18	+0.23	+0.68	+0.21	1		Preston et al. (2006)	
CS 22880–074	5621	3.50	0.80	−2.29	−0.10	+1.30	0.00	+1.30	+0.24	+1.31	CEMP-s/rs	0		Yong et al. (2013)
CS 22880–086	5196	2.54	1.62	−3.05	...	+0.24	+0.01	+0.25	−0.03	−0.85	1		Yong et al. (2013)	
CS 22881–036	6200	4.00	0.47	−2.00	...	+2.04	0.00	+2.04	+0.69	+1.84	CEMP-s/rs	0		Preston & Sneden (2001)
CS 22882–001	5950	2.50	1.89	−2.49	...	+0.06	+0.01	+0.07	+0.29	+0.13	1		Preston et al. (2006)	
CS 22885–096	4992	1.93	2.16	−3.86	\leq +0.26	+0.26	+0.01	+0.27	−1.26	−1.10	1		Yong et al. (2013)	
CS 22886–042	4798	1.48	2.54	−2.83	\leq +2.03	+0.12	+0.44	+0.56	−0.07	−0.32	1		Yong et al. (2013)	
CS 22888–031	6241	4.47	0.01	−3.31	...	+0.38	0.00	+0.38	+0.28	...	1		Yong et al. (2013)	
CS 22891–171	5100	1.60	2.53	−2.25	+1.67	+1.56	+0.12	+1.68	...	+2.48	CEMP-s/rs	0		Allen et al. (2012)
CS 22891–184	5600	2.20	2.09	−2.59	...	+0.26	+0.01	+0.27	+0.09	−0.08	1		Preston et al. (2006)	
CS 22891–200	4490	0.50	3.40	−3.47	+1.20	+0.64	+0.73	+1.37	−1.32	−0.93	CEMP-no	1		McWilliam et al. (1995)
CS 22891–209	4699	1.18	2.80	−3.32	+1.12	−0.65	+0.69	+0.04	+0.18	−0.55	1		Yong et al. (2013)	
CS 22892–052	4710	1.50	2.49	−3.10	+1.00	+1.05	+0.38	+1.43	+0.68	+0.96	CEMP	0		Masseron et al. (2012)
CS 22893–010	5150	2.45	1.69	−2.93	+1.55	+0.13	+0.01	+0.14	+0.01	−1.28	1		Roederer et al. (2014)	
CS 22896–154	5100	2.28	1.85	−2.85	−0.23	+0.23	+0.01	+0.24	+0.63	+0.51	1		Yong et al. (2013)	
CS 22897–008	4795	1.43	2.59	−3.50	+0.24	+0.56	+0.45	+1.01	+0.55	−1.00	CEMP-no	1		Yong et al. (2013)
CS 22898–027	6250	3.70	0.78	−2.26	+0.90	+2.20	0.00	+2.20	+0.98	+2.23	CEMP-s/rs	0		Masseron et al. (2012)
CS 22937–072	5450	2.10	2.14	−2.74	...	+0.51	+0.02	+0.53	+0.17	−0.18	1		Preston et al. (2006)	
CS 22941–012	7200	4.20	0.53	−2.02	+0.09	+0.09	0.00	+0.09	+0.29	+0.01	1		Sneden et al. (2003)	
CS 22942–019	5000	2.40	1.69	−2.64	...	+2.00	+0.02	+2.02	+1.50	+1.92	CEMP-s/rs	0		Aoki et al. (2002)
CS 22943–132	5850	3.60	0.76	−2.67	+0.49	+0.69	0.00	+0.69	...	−0.05	1		Roederer et al. (2014)	
CS 22943–201	5970	2.45	1.95	−2.69	+1.56	+1.89	+0.02	+1.91	...	−0.53	CEMP-no	1		Roederer et al. (2014)
CS 22944–032	5293	2.82	1.37	−2.98	\leq −0.44	+0.31	+0.01	+0.32	−0.24	−0.76	1		Yong et al. (2013)	
CS 22944–039	5350	1.50	2.71	−2.41	...	−0.22	+0.49	+0.27	+0.47	−0.19	1		Preston et al. (2006)	
CS 22945–024	5120	2.35	1.78	−2.58	+0.26	+2.31	+0.02	+2.33	+0.30	+1.44	CEMP-s/rs	0		Roederer et al. (2014)
CS 22945–028	5126	2.55	1.59	−2.66	...	+0.17	+0.01	+0.18	+0.16	−0.18	1		Barklem et al. (2005)	
CS 22947–187	5200	1.50	2.66	−2.51	+1.73	+1.07	+0.27	+1.34	+0.58	+1.24	CEMP-s/rs	0		Masseron et al. (2012)
CS 22948–006	5550	1.95	2.32	−2.62	...	+0.49	+0.08	+0.57	−0.22	−0.68	1		Preston et al. (2006)	
CS 22948–027	4600	1.00	2.95	−2.57	+1.80	+2.00	+0.14	+2.14	+0.95	+1.85	CEMP-s/rs	0		Masseron et al. (2012)
CS 22948–066	4830	1.55	2.48	−3.18	+1.05	−0.74	+0.36	−0.38	−0.35	−1.15	1		Roederer et al. (2014)	
CS 22948–104	5000	2.30	1.79	−2.76	...	+0.38	+0.01	+0.39	1		Masseron et al. (2012)	
CS 22949–008a	6300	3.50	0.99	−2.09	+0.41	+1.55	0.00	+1.55	...	+1.32	CEMP-s/rs	0		Masseron et al. (2012)
CS 22949–008b	5300	4.70	−0.51	−2.09	+0.41	+1.55	0.00	+1.55	...	+1.32	CEMP-s/rs	0		Masseron et al. (2012)
CS 22949–037	4630	0.95	3.01	−4.21	+2.50	+0.99	+0.74	+1.73	...	−0.78	CEMP-no	1		Roederer et al. (2014)
CS 22949–048	4828	1.81	2.22	−2.73	...	−0.24	+0.14	−0.10	−1.47	\leq −1.38	1		Lai et al. (2007)	
CS 22950–046	4769	1.37	2.64	−3.39	...	−0.50	+0.52	+0.02	−0.62	−1.23	1		Yong et al. (2013)	
CS 22951–077	5350	1.75	2.46	−2.43	...	−0.10	+0.25	+0.15	−0.02	−0.34	1		Preston et al. (2006)	
CS 22952–015	4824	1.50	2.53	−3.44	+1.31	−0.41	+0.38	−0.03	−0.87	−1.33	1		Yong et al. (2013)	
CS 22953–003	5002	2.01	2.08	−2.93	+0.12	+0.30	+0.02	+0.32	+0.33	+0.49	1		Yong et al. (2013)	
CS 22953–037	6627	4.11	0.47	−2.70	...	+0.37	0.00	+0.37	\leq −1.20	\leq −0.25	1		Yong et al. (2013)	
CS 22956–050	4844	1.56	2.48	−3.39	+0.31	+0.27	+0.33	+0.60	−0.33	−0.78	1		Yong et al. (2013)	

Table 3 — *Continued*

Name	T_{eff} (K)	$\log g$ (cgs)	$\log L$ (L_{\odot})	[Fe/H]	[N/Fe]	[C/Fe]	$\Delta[\text{C}/\text{Fe}]$ ([N/Fe]=0)	$[\text{C}/\text{Fe}]_c$	[Sr/Fe]	[Ba/Fe]	Class	I/O	Ref.
CS 22957–013	4904	1.96	2.10	−2.64	...	+0.06	+0.06	+0.12	−0.17	−0.60		1	Barklem et al. (2005)
CS 22957–022	5146	2.40	1.74	−2.92	+0.21	+0.16	+0.01	+0.17	−0.31	−1.09		1	Yong et al. (2013)
CS 22957–027	5220	2.65	1.52	−3.00	+1.50	+2.42	+0.02	+2.44	...	−1.00	CEMP-no	1	Roederer et al. (2014)
CS 22958–042	5760	3.55	0.79	−2.99	+2.25	+2.15	0.00	+2.15	−0.52	−1.02	CEMP-no	1	Roederer et al. (2014)
CS 22958–083	4900	1.90	2.16	−2.97	...	+0.71	+0.07	+0.78	−0.14	≤ −0.82	CEMP-no	1	Preston et al. (2006)
CS 22960–010	5737	4.85	−0.52	−2.65	...	+0.78	0.00	+0.78	CEMP	1	Barklem et al. (2005)
CS 22960–053	5200	2.10	2.06	−3.14	...	+2.05	+0.02	+2.07	...	+0.86	CEMP	0	Aoki et al. (2007)
CS 22960–064	5060	2.20	1.91	−2.77	+1.35	+0.14	+0.01	+0.15	...	−0.20		1	Roederer et al. (2014)
CS 22963–004	5597	3.34	0.95	−3.54	+0.80	+0.40	0.00	+0.40	−0.73	−0.51		1	Yong et al. (2013)
CS 22964–161a	6050	3.70	0.72	−2.37	...	+1.58	0.00	+1.58	+0.55	+1.36	CEMP-s/rs	0	Thompson et al. (2008)
CS 22964–161b	5850	4.10	0.26	−2.39	...	+1.40	0.00	+1.40	+0.45	+1.30	CEMP-s/rs	0	Thompson et al. (2008)
CS 22964–214	6180	3.75	0.71	−2.95	+1.51	+0.62	0.00	+0.62	−0.25	−0.54		1	Roederer et al. (2014)
CS 22965–016	4904	1.99	2.07	−2.42	...	−0.74	+0.04	−0.70	+0.12	≤ −1.07		1	Lai et al. (2007)
CS 22965–029	5467	3.38	0.87	−2.14	...	−0.64	0.00	−0.64	+0.64	+0.16		1	Lai et al. (2007)
CS 22965–054	6137	3.68	0.77	−3.10	...	+0.62	0.00	+0.62	+0.19	≤ −0.48		1	Yong et al. (2013)
CS 22966–011	6298	4.43	0.06	−3.02	...	+0.45	0.00	+0.45	+0.13	−0.05		1	Yong et al. (2013)
CS 22966–057	5364	3.07	1.14	−2.43	+0.10	+0.06	+0.01	+0.07	−0.01	−0.24		1	Yong et al. (2013)
CS 22968–001	6000	4.00	0.41	−3.01	...	+0.48	0.00	+0.48	−0.23	−0.69		1	Preston et al. (2006)
CS 22968–014	4864	1.60	2.44	−3.58	+0.24	+0.25	+0.25	+0.50	−1.69	−1.77		1	Yong et al. (2013)
CS 29491–053	4700	1.21	2.77	−3.03	+0.82	−0.27	+0.66	+0.39	−0.15	−0.89		1	Yong et al. (2013)
CS 29491–069	5103	2.45	1.68	−2.81	...	+0.14	+0.01	+0.15	+0.29	+0.32		1	Barklem et al. (2005)
CS 29491–109	4736	1.50	2.50	−2.90	...	−0.23	+0.43	+0.20	−0.28	−0.97		1	Barklem et al. (2005)
CS 29493–090	4692	1.28	2.70	−3.13	+0.76	+0.70	+0.53	+1.23	...	+0.52	CEMP	1	Barklem et al. (2005)
CS 29495–041	4740	1.34	2.66	−2.74	+0.40	−0.07	+0.55	+0.48	−0.06	−0.65		1	Yong et al. (2013)
CS 29497–004	5013	2.23	1.87	−2.81	...	+0.18	+0.01	+0.19	+0.67	+1.16		0	Barklem et al. (2005)
CS 29497–030	6650	3.50	1.09	−2.70	+1.88	+2.38	+0.01	+2.39	+1.37	+2.17	CEMP-s/rs	0	Masseron et al. (2012)
CS 29497–034	4983	1.96	2.13	−3.00	+2.63	+2.72	+0.04	+2.76	+1.05	+2.28	CEMP-s/rs	0	Yong et al. (2013)
CS 29497–040	5487	3.41	0.84	−2.63	...	+0.31	0.00	+0.31	≤ +0.03	≤ −0.89		1	Lai et al. (2007)
CS 29498–043	4440	0.50	3.39	−3.85	+1.71	+2.72	+0.31	+3.03	−0.30	−0.51	CEMP-no	1	Roederer et al. (2014)
CS 29499–060	6595	4.05	0.52	−2.50	...	+0.38	0.00	+0.38	−0.40	≤ −0.51		1	Yong et al. (2013)
CS 29502–042	5039	2.09	2.02	−3.27	−0.43	+0.16	+0.01	+0.17	−1.88	−1.69		1	Yong et al. (2013)
CS 29502–092	4820	1.50	2.53	−3.20	+1.00	+0.96	+0.39	+1.35	−0.30	−1.46	CEMP-no	1	Roederer et al. (2014)
CS 29506–007	6522	3.94	0.61	−2.73	≤ +0.93	+0.49	0.00	+0.49	+0.18	+0.09		1	Yong et al. (2013)
CS 29506–090	6603	4.18	0.39	−2.62	...	+0.41	0.00	+0.41	+0.46	−0.35		1	Yong et al. (2013)
CS 29509–027	6850	3.50	1.14	−2.42	+2.44	+1.74	0.00	+1.74	+1.03	+1.50	CEMP-s/rs	0	Roederer et al. (2014)
CS 29510–058	5192	2.73	1.43	−2.34	...	+0.46	+0.01	+0.47	+0.27	−0.14		1	Lai et al. (2007)
CS 29512–073	5600	3.40	0.89	−2.04	+0.56	+1.20	0.00	+1.20	...	+1.12	CEMP-s/rs	0	Masseron et al. (2012)
CS 29513–032	5810	3.30	1.05	−2.08	...	+0.63	0.00	+0.63		1	Roederer et al. (2010)
CS 29516–024	4637	1.04	2.92	−3.05	−0.76	−0.06	+0.74	+0.68	−0.48	−0.90		1	Yong et al. (2013)
CS 29517–025	5647	3.53	0.77	−2.02	...	−0.39	0.00	−0.39	+0.77	+0.71		0	Lai et al. (2007)
CS 29518–051	5100	2.29	1.84	−2.64	+0.82	−0.13	+0.01	−0.12	+0.15	−0.45		1	Yong et al. (2013)
CS 29522–046	5974	3.72	0.68	−2.12	−0.33	+0.42	0.00	+0.42	+0.16	−0.13		1	Yong et al. (2013)
CS 29526–110	6800	4.10	0.53	−2.38	+1.49	+2.29	0.00	+2.29	+0.93	+2.15	CEMP-s/rs	0	Aoki et al. (2008)
CS 29527–015	6577	3.89	0.68	−3.32	...	+1.18	0.00	+1.18	+0.44	...	CEMP	1	Yong et al. (2013)
CS 29528–028	6800	4.00	0.63	−2.86	...	+2.77	0.00	+2.77	...	+3.27	CEMP-s/rs	0	Aoki et al. (2007)
CS 29528–041	6150	4.00	0.45	−3.30	+3.04	+1.57	0.00	+1.57	−0.10	+0.89	CEMP	0	Sivarani et al. (2006)
CS 30301–015	4889	1.73	2.32	−2.73	+1.70	+1.60	+0.14	+1.74	+0.37	+1.45	CEMP-s/rs	0	Yong et al. (2013)
CS 30301–024	6584	4.03	0.54	−2.54	...	+0.23	0.00	+0.23	...	−0.28		1	Yong et al. (2013)
CS 30306–082	5598	3.50	0.79	−2.43	...	+0.21	0.00	+0.21	−0.22	−0.41		1	Lai et al. (2007)
CS 30306–132	5047	2.16	1.95	−2.56	...	+0.34	+0.01	+0.35	+0.18	+0.22		1	Yong et al. (2013)
CS 30308–035	4806	1.78	2.24	−3.35	...	0.00	+0.09	+0.09	−0.71	...		1	Barklem et al. (2005)
CS 30312–059	4908	1.75	2.31	−3.22	≤ −0.48	+0.27	+0.11	+0.38	+0.02	−0.14		1	Yong et al. (2013)
CS 30312–100	5117	2.34	1.79	−2.66	≤ +1.85	+0.54	+0.01	+0.55	...	−0.73		1	Yong et al. (2013)
CS 30314–067	4320	0.50	3.34	−3.01	+1.18	+0.55	+0.66	+1.21	−0.27	−0.55	CEMP-no	1	Roederer et al. (2014)
CS 30315–001	4565	1.14	2.79	−2.97	...	−0.54	+0.72	+0.18	+0.42	−0.87		1	Barklem et al. (2005)

Table 3 — *Continued*

Name	T_{eff} (K)	$\log g$ (cgs)	$\log L$ (L_{\odot})	[Fe/H]	[N/Fe]	[C/Fe]	$\Delta[\text{C}/\text{Fe}]$ ([N/Fe]=0)	$[\text{C}/\text{Fe}]_c$	[Sr/Fe]	[Ba/Fe]	Class	I/O	Ref.
CS 30315–029	4541	1.07	2.85	−3.33	...	−0.47	+0.75	+0.28	−0.09	+0.36	1	Barklem et al. (2005)	
CS 30315–093	5638	3.52	0.78	−2.39	...	−0.09	0.00	−0.09	−0.11	−0.52	1	Lai et al. (2007)	
CS 30319–020	5200	2.50	1.66	−2.35	...	+0.32	+0.01	+0.33	−0.01	−0.73	1	Aoki et al. (2005)	
CS 30325–028	4894	1.73	2.32	−2.87	−0.22	+0.38	+0.21	+0.59	+0.19	−0.49	1	Yong et al. (2013)	
CS 30325–094	4948	1.85	2.22	−3.35	+0.18	0.00	+0.04	+0.04	−2.14	−1.88	1	Yong et al. (2013)	
CS 30327–038	5100	1.70	2.43	−2.64	...	−0.19	+0.27	+0.08	−0.59	−1.46	1	Aoki et al. (2005)	
CS 30329–004	5000	1.50	2.59	−2.75	...	−0.28	+0.46	+0.18	+0.07	−0.89	1	Aoki et al. (2005)	
CS 30329–129	5467	3.37	0.88	−2.24	...	+0.11	0.00	+0.11	+0.04	−0.60	1	Lai et al. (2007)	
CS 30336–049	4827	1.51	2.52	−4.03	+1.00	−0.20	+0.29	+0.09	−1.53	−1.50	1	Lai et al. (2008)	
CS 30337–097	4865	1.81	2.23	−2.74	...	−0.08	+0.15	+0.07	1	Barklem et al. (2005)	
CS 30338–089	4886	1.72	2.33	−2.78	+1.27	+2.06	+0.11	+2.17	...	+2.30	CEMP-s/rs	0	Yong et al. (2013)
CS 30339–041	5478	2.10	2.15	−2.21	...	−0.45	+0.01	−0.44	+0.25	+0.07	1	Barklem et al. (2005)	
CS 30339–069	6326	3.79	0.71	−3.05	...	+0.56	0.00	+0.56	−0.00	...	1	Yong et al. (2013)	
CS 30343–063	4412	0.83	3.04	−2.97	...	−0.71	+0.75	+0.04	+0.05	−0.95	1	Barklem et al. (2005)	
CS 30492–001	5790	3.65	0.70	−2.35	+1.12	−0.05	0.00	−0.05	...	−0.45	1	Roederer et al. (2014)	
CS 31060–047	4749	1.55	2.45	−2.72	...	−0.30	+0.41	+0.11	−0.04	−1.07	1	Barklem et al. (2005)	
CS 31061–032	6448	4.33	0.20	−2.56	...	+0.56	0.00	+0.56	+0.31	−0.40	1	Yong et al. (2013)	
CS 31062–012	6190	4.47	−0.01	−2.67	+1.20	+2.12	0.00	+2.12	...	+2.32	CEMP-s/rs	0	Yong et al. (2013)
CS 31062–041	4990	2.00	2.09	−2.65	\leq +1.59	+0.58	+0.04	+0.62	−0.29	−0.42	1	Yong et al. (2013)	
CS 31062–050	5607	3.49	0.80	−2.28	+1.20	+2.00	0.00	+2.00	...	+2.30	CEMP-s/rs	0	Yong et al. (2013)
CS 31069–064	5468	3.38	0.87	−2.02	...	+0.16	0.00	+0.16	−0.53	−0.90	1	Lai et al. (2007)	
CS 31070–058	4864	1.89	2.15	−2.12	...	+0.11	+0.14	+0.25	+0.17	−0.21	1	Lai et al. (2007)	
CS 31072–118	4606	1.25	2.70	−3.06	...	−0.54	+0.65	+0.11	−0.07	−1.09	1	Barklem et al. (2005)	
CS 31078–018	5100	2.27	1.86	−2.99	−0.38	+0.37	+0.01	+0.38	+0.26	+0.38	1	Yong et al. (2013)	
CS 31080–095	6050	4.50	−0.08	−2.85	+0.67	+2.67	0.00	+2.67	−0.31	+0.72	CEMP	0	Sivarani et al. (2006)
CS 31082–001	4866	1.66	2.38	−2.75	−0.51	+0.16	+0.30	+0.46	+0.75	+1.02	0	Yong et al. (2013)	
CS 31085–024	5778	4.64	−0.30	−2.80	\leq −0.24	+0.36	0.00	+0.36	−0.24	−0.57	1	Yong et al. (2013)	
G 64–37	6318	4.16	0.34	−3.12	...	+0.25	0.00	+0.25	1	Simmerer et al. (2004)	
G 77–61	4000	5.00	−1.30	−4.03	+2.48	+2.49	0.00	+2.49	...	\leq +1.00	CEMP-no	1	Masseron et al. (2012)
HD 2796	4923	1.84	2.22	−2.31	+0.85	−0.50	+0.17	−0.33	+0.33	−0.14	1	Yong et al. (2013)	
HD 3008	4250	1.03	2.78	−2.08	...	−0.29	+0.65	+0.36	...	+0.08	1	Simmerer et al. (2004)	
HD 4306	4854	1.61	2.43	−3.04	...	+0.11	+0.31	+0.42	−0.07	−1.17	1	Yong et al. (2013)	
HD 5223	4500	1.00	2.91	−2.11	...	+1.58	+0.12	+1.70	+1.49	+1.88	CEMP-s/rs	0	Goswami et al. (2006)
HD 5426	4910	1.90	2.16	−2.39	...	−0.04	+0.12	+0.08	+0.24	−0.14	1	McWilliam et al. (1995)	
HD 6268	4696	1.23	2.75	−2.74	...	−0.67	+0.68	+0.01	+0.11	−0.04	1	Yong et al. (2013)	
HD 13979	4970	1.15	2.93	−2.63	...	−0.50	+0.70	+0.20	−0.91	−0.73	1	McWilliam et al. (1995)	
HD 23798	4450	1.06	2.83	−2.26	...	−0.59	+0.74	+0.15	1	Simmerer et al. (2004)	
HD 26169	4750	1.35	2.65	−2.80	−0.45	+0.15	+0.54	+0.69	+0.44	−0.50	1	Roederer et al. (2014)	
HD 29574	4250	0.80	3.01	−2.00	...	−0.69	+0.71	+0.02	...	+0.59	1	Simmerer et al. (2004)	
HD 85773	4268	0.87	2.95	−2.62	...	−0.49	+0.75	+0.26	...	−0.49	1	Simmerer et al. (2004)	
HD 88609	4541	0.80	3.12	−2.98	...	−0.51	+0.75	+0.24	−0.01	−1.05	1	Yong et al. (2013)	
HD 103036	4200	1.14	2.65	−2.04	...	−0.39	+0.63	+0.24	1	Simmerer et al. (2004)	
HD 103545	4666	1.64	2.33	−2.45	...	−0.44	+0.37	−0.07	...	−0.04	1	Simmerer et al. (2004)	
HD 107752	4649	1.63	2.34	−2.78	...	−0.59	+0.32	−0.27	...	−0.24	1	Simmerer et al. (2004)	
HD 108317	5234	2.68	1.49	−2.18	...	−0.09	+0.01	−0.08	...	+0.58	1	Simmerer et al. (2004)	
HD 110184	4250	0.79	3.02	−2.72	...	−0.34	+0.75	+0.41	−0.02	−0.01	1	Simmerer et al. (2004)	
HD 115444	4711	1.23	2.76	−2.65	...	−0.41	+0.66	+0.25	+0.32	+0.14	1	Yong et al. (2013)	
HD 119516	5382	2.47	1.75	−2.11	...	−1.19	+0.01	−1.18	1	Simmerer et al. (2004)	
HD 122563	4843	1.62	2.42	−2.54	+0.70	−0.44	+0.36	−0.08	−0.38	−1.12	1	Yong et al. (2013)	
HD 126587	4853	1.61	2.43	−3.00	...	+0.19	+0.31	+0.50	−0.09	−0.10	1	Yong et al. (2013)	
HD 128279	5050	2.15	1.96	−2.52	−0.39	+0.08	+0.01	+0.09	−0.51	−0.64	1	Roederer et al. (2014)	
HD 135148	4183	1.24	2.54	−2.17	...	+0.76	+0.34	+1.10	...	+0.30	CEMP	1	Simmerer et al. (2004)
HD 140283	5711	3.53	0.79	−2.56	...	+0.28	0.00	+0.28	−0.05	−0.94	1	Yong et al. (2013)	
HD 165195	4237	0.78	3.02	−2.60	...	−0.54	+0.75	+0.21	+0.11	+0.23	1	Simmerer et al. (2004)	
HD 178443	5180	1.65	2.50	−2.05	...	−0.28	+0.35	+0.07	+0.27	+0.01	1	McWilliam et al. (1995)	

Table 3 — *Continued*

Name	T_{eff} (K)	$\log g$ (cgs)	$\log L$ (L_{\odot})	[Fe/H]	[N/Fe]	[C/Fe]	$\Delta[\text{C}/\text{Fe}]$ ([N/Fe]=0)	[C/Fe] _c	[Sr/Fe]	[Ba/Fe]	Class	I/O	Ref.
HD 186478	4629	1.07	2.89	-2.68	+0.62	-0.28	+0.73	+0.45	+0.32	-0.04		1	Yong et al. (2013)
HD 196944	5255	2.74	1.44	-2.44	+1.30	+1.20	+0.02	+1.22	+0.89	+1.10	CEMP- <i>s/rs</i>	0	Yong et al. (2013)
HD 200654	5160	2.55	1.60	-2.80	...	+0.27	+0.01	+0.28	-0.44	-0.83		1	McWilliam et al. (1995)
HD 214925	4050	0.30	3.43	-2.03	...	-0.85	+0.74	-0.11		1	Aoki et al. (2008)
HD 215801	6005	3.81	0.60	-2.29	...	+0.04	0.00	+0.04		1	Akerman et al. (2004)
HD 216143	4450	0.80	3.09	-2.27	...	-0.41	+0.73	+0.32	+0.21	-0.27		1	Aoki et al. (2008)
HD 237846	4600	1.00	2.95	-3.29	...	+0.17	+0.75	+0.92	CEMP	1	Roederer et al. (2010)
HD 340279	6273	4.25	0.24	-2.62	...	+0.17	0.00	+0.17		1	Akerman et al. (2004)
HE 0005–0002	4726	1.58	2.41	-3.06	...	+0.13	+0.32	+0.45	+0.29	-0.03		1	Barklem et al. (2005)
HE 0007–1832	6500	3.80	0.75	-2.79	+2.11	+2.66	0.00	+2.66	+0.22	+0.09	CEMP	1	Cohen et al. (2013)
HE 0008–3842	4327	0.65	3.19	-3.33	...	-0.93	+0.73	-0.20	-1.40	-1.80		1	Barklem et al. (2005)
HE 0009–6039	5250	2.70	1.48	-3.29	...	+0.16	+0.01	+0.17	...	-1.11		1	Cohen et al. (2013)
HE 0011–0035	4950	1.80	2.27	-2.99	...	0.00	+0.12	+0.12	...	-0.27		1	Cohen et al. (2013)
HE 0012–1441	5750	3.50	0.83	-2.52	+0.54	+1.59	0.00	+1.59	...	+1.15	CEMP- <i>s/rs</i>	0	Cohen et al. (2013)
HE 0013–0257	4500	0.50	3.41	-3.82	...	-0.22	+0.69	+0.47	...	-1.16		1	Hollek et al. (2011)
HE 0013–0522	4900	1.70	2.36	-3.24	...	+0.22	+0.15	+0.37	...	-0.89		1	Hollek et al. (2011)
HE 0015+0048	4600	0.90	3.05	-3.07	...	+0.62	+0.67	+1.29	...	-1.17	CEMP-no	1	Hollek et al. (2011)
HE 0017–4346	6198	3.80	0.66	-3.07	...	+2.90	0.00	+2.90	...	+1.28	CEMP- <i>s/rs</i>	0	Cohen et al. (2013)
HE 0017–4838	5149	2.23	1.91	-3.23	...	-0.33	0.00	-0.33	+0.78	-0.83		1	Barklem et al. (2005)
HE 0018–1349	5719	4.62	-0.29	-2.27	...	+0.32	0.00	+0.32	+0.05	+0.43		1	Barklem et al. (2005)
HE 0023–4825	5816	3.63	0.72	-2.06	...	+0.27	0.00	+0.27	+0.08	-0.11		1	Barklem et al. (2005)
HE 0024–2523	6625	4.30	0.28	-2.70	+2.12	+2.62	0.00	+2.62	+0.44	+1.52	CEMP- <i>s/rs</i>	0	Masseron et al. (2012)
HE 0029–1839	5010	2.19	1.91	-2.50	...	+0.27	+0.01	+0.28	+0.13	-1.35		1	Barklem et al. (2005)
HE 0037–0348	4920	1.80	2.26	-3.15	+0.92	+0.12	+0.10	+0.22	...	-0.52		1	Cohen et al. (2013)
HE 0037–2657	4982	2.21	1.88	-3.22	...	+0.27	+0.01	+0.28	-0.54	-1.14		1	Barklem et al. (2005)
HE 0039–4154	4784	1.50	2.52	-3.18	...	+0.06	+0.38	+0.44	-0.14	+0.02		1	Cohen et al. (2013)
HE 0043–2845	5517	4.42	-0.16	-2.91	...	+0.15	0.00	+0.15	-0.67	...		1	Barklem et al. (2005)
HE 0044–2459	5242	2.92	1.25	-3.28	...	+0.41	0.00	+0.41	-1.55	...		1	Barklem et al. (2005)
HE 0044–4023	5694	3.26	1.06	-2.56	...	+0.36	0.00	+0.36	+0.03	-0.40		1	Barklem et al. (2005)
HE 0048–0611	5180	2.50	1.65	-2.66	+0.13	+0.37	+0.01	+0.38	...	-0.43		1	Cohen et al. (2013)
HE 0048–6408	4360	0.35	3.50	-3.76	...	-0.30	+0.69	+0.39	-0.82	-1.37		1	Placco et al. (2014a)
HE 0049–5700	5952	4.08	0.31	-2.40	...	+0.35	0.00	+0.35	+0.19	-0.47		1	Barklem et al. (2005)
HE 0051–2304	4537	1.22	2.70	-2.44	...	-0.68	+0.69	+0.01	+0.03	-0.11		1	Barklem et al. (2005)
HE 0054–0657	5908	4.40	-0.02	-2.00	...	+0.25	0.00	+0.25	+0.05	-0.13		1	Barklem et al. (2005)
HE 0055–2314	6290	4.40	0.09	-2.66	...	+0.72	0.00	+0.72	...	-0.49	CEMP-no	1	Cohen et al. (2013)
HE 0057–4541	5083	2.55	1.57	-2.31	...	+0.13	+0.01	+0.14	+0.16	-0.16		1	Barklem et al. (2005)
HE 0057–5959	5257	2.65	1.53	-4.08	+2.15	+0.86	0.00	+0.86	...	-0.46	CEMP-no	1	Yong et al. (2013)
HE 0058–0244	5620	3.40	0.89	-2.76	+1.78	+1.93	+0.01	+1.94	+0.42	+1.97	CEMP- <i>s/rs</i>	0	Cohen et al. (2013)
HE 0102–0633	6012	3.70	0.71	-3.10	...	+0.87	0.00	+0.87	-0.41	-0.54	CEMP-no	1	Cohen et al. (2013)
HE 0102–1213	6100	3.65	0.79	-3.28	...	+1.31	0.00	+1.31	...	≤ -0.64	CEMP-no	1	Yong et al. (2013)
HE 0103–0357	5406	3.20	1.03	-3.15	-0.03	+0.52	0.00	+0.52	...	-0.87		1	Cohen et al. (2013)
HE 0104–4007	5154	2.64	1.50	-3.30	...	+0.46	+0.01	+0.47	-0.88	-0.69		1	Barklem et al. (2005)
HE 0104–5300	4732	1.43	2.57	-3.31	...	-0.05	+0.45	+0.40	-0.49	-1.57		1	Barklem et al. (2005)
HE 0105–6141	5218	2.83	1.34	-2.55	...	+0.16	+0.01	+0.17	+0.08	+0.13		1	Barklem et al. (2005)
HE 0107–5240	5100	2.20	1.93	-5.54	+2.43	+3.85	+0.06	+3.91	≤ -0.20	≤ +0.82	CEMP-no	1	Yong et al. (2013)
HE 0109–0742	5315	1.85	2.35	-2.52	...	-0.18	+0.15	-0.03	+0.07	-0.22		1	Barklem et al. (2005)
HE 0111–1454	4632	1.05	2.91	-2.99	...	-0.26	+0.74	+0.48	-0.03	-0.75		1	Barklem et al. (2005)
HE 0121–2826	4955	1.99	2.09	-2.97	...	+0.46	+0.03	+0.49	+0.37	-0.64		1	Barklem et al. (2005)
HE 0122–1616	5215	2.50	1.66	-2.80	...	+0.31	+0.01	+0.32	...	-1.07		1	Cohen et al. (2013)
HE 0130–1749	4820	1.60	2.43	-3.34	...	+0.40	+0.32	+0.72	...	-0.72	CEMP-no	1	Cohen et al. (2013)
HE 0131–2740	5351	3.03	1.18	-3.08	...	+0.31	0.00	+0.31		1	Barklem et al. (2005)
HE 0131–3953	5928	3.83	0.56	-2.71	...	+2.36	0.00	+2.36	+0.56	+2.12	CEMP- <i>s/rs</i>	0	Barklem et al. (2005)
HE 0132–2429	5294	2.75	1.44	-3.60	+1.22	+0.83	+0.01	+0.84	+0.13	-0.85	CEMP-no	1	Cohen et al. (2008)
HE 0132–2439	5249	2.63	1.55	-3.79	+1.07	+0.62	+0.01	+0.63	...	-0.88		1	Yong et al. (2013)
HE 0134–1519	5525	3.17	1.10	-3.98	≤ -0.20	+1.00	0.00	+1.00	...	≤ -0.81	CEMP-no	1	Hansen et al. (2014)

Table 3 — *Continued*

Name	T_{eff} (K)	$\log g$ (cgs)	$\log L$ (L_{\odot})	[Fe/H]	[N/Fe]	[C/Fe]	$\Delta[\text{C}/\text{Fe}]$ ([N/Fe]=0)	$[\text{C}/\text{Fe}]_c$	[Sr/Fe]	[Ba/Fe]	Class	I/O	Ref.
HE 0134–2504	5204	2.50	1.66	−2.74	...	+1.79	+0.02	+1.81	...	+1.65	CEMP-s/rs	0	Cohen et al. (2013)
HE 0139–2826	4900	1.50	2.56	−3.46	+0.03	+0.48	+0.38	+0.86	−1.51	−1.22	CEMP-no	1	Placco et al. (2014a)
HE 0143–0441	6276	3.84	0.65	−2.32	+0.85	+1.82	0.00	+1.82	+0.93	+2.42	CEMP-s/rs	0	Yong et al. (2013)
HE 0143–1135	5629	4.53	−0.23	−2.13	...	+0.19	0.00	+0.19	−0.10	−0.13		1	Barklem et al. (2005)
HE 0143–4108	5121	2.41	1.72	−2.62	...	+0.12	+0.01	+0.13	−0.84	−1.23		1	Barklem et al. (2005)
HE 0143–4146	4799	1.50	2.52	−2.95	...	+0.07	+0.41	+0.48	−0.52	−0.84		1	Barklem et al. (2005)
HE 0146–1548	4636	0.99	2.97	−3.46	...	+0.84	+0.73	+1.57	...	−0.71	CEMP-no	1	Yong et al. (2013)
HE 0157–3335	4775	1.62	2.39	−3.08	...	−0.26	+0.29	+0.03	+0.15	−0.46		1	Barklem et al. (2005)
HE 0200–0955	5216	2.57	1.60	−2.47	...	+0.37	+0.01	+0.38	−0.26	−0.73		1	Barklem et al. (2005)
HE 0206–1916	5073	2.23	1.89	−2.52	+1.61	+2.10	+0.02	+2.12	...	+1.99	CEMP-s/rs	0	Yong et al. (2013)
HE 0207–1423	5023	2.07	2.03	−2.95	...	+2.38	+0.03	+2.41	...	+1.73	CEMP-s/rs	0	Yong et al. (2013)
HE 0212–0557	5075	2.20	1.92	−2.27	+1.09	+1.74	+0.02	+1.76	+0.04	+2.18	CEMP-s/rs	0	Cohen et al. (2013)
HE 0226+0103	5250	2.70	1.48	−2.81	+0.88	+0.04	+0.01	+0.05	...	+0.12		1	Cohen et al. (2013)
HE 0231–4016	5972	3.59	0.81	−2.08	...	+1.27	0.00	+1.27	+0.77	+1.38	CEMP-s/rs	0	Barklem et al. (2005)
HE 0233–0343	6075	3.40	1.03	−4.68	$\leq +1.20$	+3.32	0.00	+3.32	...	$\leq +0.70$	CEMP-no	1	Hansen et al. (2014)
HE 0240–0807	4729	1.54	2.46	−2.68	...	−0.39	+0.42	+0.03	+0.01	+0.16		1	Barklem et al. (2005)
HE 0240–6105	4720	1.26	2.73	−3.23	...	−0.29	+0.59	+0.30	+0.46	−0.73		1	Barklem et al. (2005)
HE 0243–0753	5066	2.29	1.82	−2.49	...	+0.25	+0.01	+0.26	−0.28	−1.07		1	Barklem et al. (2005)
HE 0243–5238	5085	2.35	1.77	−3.04	...	+0.36	+0.01	+0.37	+0.06	−0.35		1	Barklem et al. (2005)
HE 0244–4111	5624	3.39	0.91	−2.56	...	+0.21	0.00	+0.21	−0.05	−0.37		1	Barklem et al. (2005)
HE 0248+0039	5199	2.57	1.59	−2.53	...	+0.05	+0.01	+0.06	−0.15	−0.31		1	Barklem et al. (2005)
HE 0251–3216	5750	3.70	0.63	−3.15	...	+2.32	0.00	+2.32	...	+1.28	CEMP-s/rs	0	Cohen et al. (2013)
HE 0255–0859	5250	4.80	−0.62	−2.55	...	−0.18	0.00	−0.18	...	−0.71		1	Cohen et al. (2013)
HE 0256–1109	5891	4.04	0.34	−2.73	...	+0.63	0.00	+0.63		1	Barklem et al. (2005)
HE 0300–0751	5280	2.97	1.22	−2.27	...	+0.06	+0.01	+0.07	+0.23	−0.02		1	Barklem et al. (2005)
HE 0302–3417a	4400	0.20	3.67	−3.70	...	+0.48	+0.72	+1.20	...	−2.10	CEMP-no	1	Hollek et al. (2011)
HE 0305–4520	4817	1.56	2.47	−2.91	...	+0.29	+0.36	+0.65	−0.56	+0.53		1	Barklem et al. (2005)
HE 0305–5442	4904	1.70	2.36	−3.30	...	+0.27	+0.16	+0.43	...	−2.41		1	Cohen et al. (2013)
HE 0308–1154	4984	2.05	2.04	−2.82	...	+0.34	+0.02	+0.36	−1.83	...		1	Barklem et al. (2005)
HE 0312–5200	5204	2.60	1.56	−3.11	...	+0.26	+0.01	+0.27	...	−0.98		1	Cohen et al. (2013)
HE 0315+0000	5013	2.11	1.99	−2.73	...	+0.14	+0.01	+0.15	+0.09	+0.30		1	Barklem et al. (2005)
HE 0316+0214	4639	1.39	2.57	−3.14	...	−0.75	+0.53	−0.22	−1.38	−1.43		1	Barklem et al. (2005)
HE 0317–0554	5400	3.10	1.13	−2.75	...	+0.40	+0.01	+0.41	...	−0.32		1	Cohen et al. (2013)
HE 0317–4640	5872	4.10	0.27	−2.32	...	+0.18	0.00	+0.18	+0.01	−0.24		1	Barklem et al. (2005)
HE 0323–4529	5127	2.51	1.63	−3.14	...	+0.34	+0.01	+0.35	+0.38	+0.25		1	Barklem et al. (2005)
HE 0324+0152a	4775	1.20	2.81	−3.32	...	+0.18	+0.66	+0.84	...	−1.20	CEMP-no	1	Hollek et al. (2011)
HE 0328–1047	5301	3.03	1.16	−2.24	...	+0.11	+0.01	+0.12	+0.11	−0.12		1	Barklem et al. (2005)
HE 0330–4004	5946	3.78	0.61	−2.19	...	+0.04	0.00	+0.04	+0.04	−0.08		1	Barklem et al. (2005)
HE 0331–4939	5206	2.60	1.56	−2.87	...	+0.30	+0.01	+0.31	+0.03	−0.98		1	Barklem et al. (2005)
HE 0332–1007	4750	1.30	2.70	−2.90	...	−0.64	+0.62	−0.02	...	−0.33		1	Cohen et al. (2013)
HE 0333–4001	5892	4.31	0.07	−2.64	...	+0.28	0.00	+0.28	−0.05	−0.21		1	Barklem et al. (2005)
HE 0336+0113	5819	3.59	0.77	−2.60	+1.60	+2.25	0.00	+2.25	+1.77	+2.69	CEMP-s/rs	0	Yong et al. (2013)
HE 0336–3829	5740	3.22	1.11	−2.75	...	+0.19	0.00	+0.19	−0.19	−0.13		1	Barklem et al. (2005)
HE 0337–5127	5247	2.86	1.32	−2.61	...	+0.12	+0.01	+0.13	+0.09	−0.07		1	Barklem et al. (2005)
HE 0338–3945	6160	4.13	0.32	−2.38	...	+2.07	0.00	+2.07	+0.84	+2.31	CEMP-s/rs	0	Jonsell et al. (2006)
HE 0340–5355	4862	1.81	2.23	−2.88	...	−0.15	+0.13	−0.02	−0.43	−1.46		1	Barklem et al. (2005)
HE 0344–0243	5140	2.30	1.84	−3.35	+0.72	−0.09	+0.01	−0.08	...	−1.23		1	Cohen et al. (2013)
HE 0347–1819	5198	4.23	−0.07	−2.77	...	−0.01	0.00	−0.01	−0.08	−0.56		1	Barklem et al. (2005)
HE 0349–0045	5022	2.30	1.80	−2.23	+0.50	+0.15	+0.01	+0.16	...	−1.56		1	Cohen et al. (2013)
HE 0353–6024	5320	3.15	1.05	−3.17	...	+0.25	0.00	+0.25	−1.18	...		1	Barklem et al. (2005)
HE 0400–2917	5065	2.39	1.72	−2.88	...	+0.11	+0.01	+0.12	−0.77	−1.14		1	Barklem et al. (2005)
HE 0401–0138	4866	1.76	2.28	−3.34	...	+0.20	+0.12	+0.32	+0.21	−0.25		1	Barklem et al. (2005)
HE 0401–3835	5458	3.20	1.04	−3.05	...	+0.78	0.00	+0.78	...	−0.75	CEMP-no	1	Cohen et al. (2013)
HE 0411–5725	5000	2.10	1.99	−3.08	...	+0.35	+0.01	+0.36	...	−1.25		1	Cohen et al. (2013)
HE 0414–0343	4660	0.75	3.22	−2.38	...	+1.38	+0.21	+1.59	...	+1.73	CEMP-s/rs	0	Hollek et al. (2014)

Table 3 — *Continued*

Name	T_{eff} (K)	$\log g$ (cgs)	$\log L$ (L_{\odot})	[Fe/H]	[N/Fe]	[C/Fe]	$\Delta[\text{C}/\text{Fe}]$ ([N/Fe]=0)	$[\text{C}/\text{Fe}]_c$	[Sr/Fe]	[Ba/Fe]	Class	I/O	Ref.
HE 0417–0821	5811	4.83	−0.48	−2.33	...	+0.21	0.00	+0.21	−0.06	−0.41	1	Barklem et al. (2005)	
HE 0420+0123a	4800	1.45	2.57	−3.03	...	+0.33	+0.45	+0.78	...	+0.08	CEMP	1	Hollek et al. (2011)
HE 0430–4404	6214	4.27	0.20	−2.07	...	+1.35	0.00	+1.35	+0.66	+1.53	CEMP- <i>s/rs</i>	0	Barklem et al. (2005)
HE 0430–4901	5296	3.12	1.07	−2.72	...	+0.05	+0.01	+0.06	+0.10	+0.46	1	Barklem et al. (2005)	
HE 0432–0923	5131	2.64	1.50	−3.19	...	+0.20	+0.01	+0.21	+0.58	+0.67	0	Barklem et al. (2005)	
HE 0432–1005a	4525	0.50	3.42	−3.21	...	+0.23	+0.73	+0.96	...	−0.90	CEMP-no	1	Hollek et al. (2011)
HE 0436–4008	5431	3.34	0.90	−2.35	...	+0.45	0.00	+0.45	+0.43	−0.31	1	Barklem et al. (2005)	
HE 0441–0652	4811	1.52	2.50	−2.77	+0.89	+1.38	+0.25	+1.63	...	+1.20	CEMP- <i>s/rs</i>	0	Yong et al. (2013)
HE 0441–4343	5629	3.59	0.71	−2.52	...	+0.29	0.00	+0.29	−0.01	−0.65	1	Barklem et al. (2005)	
HE 0442–1234	4604	1.34	2.61	−2.41	...	−0.65	+0.61	−0.04	−0.22	−0.19	1	Barklem et al. (2005)	
HE 0445–2339	5165	2.10	2.05	−2.85	...	−0.57	0.00	−0.57	...	−0.64	1	Cohen et al. (2013)	
HE 0447–1858	5570	3.50	0.78	−2.56	−1.12	+0.17	0.00	+0.17	...	−1.61	1	Cohen et al. (2013)	
HE 0450–4705	5429	3.34	0.89	−3.10	...	+0.80	0.00	+0.80	−0.38	...	CEMP	1	Barklem et al. (2005)
HE 0454–4758	5388	3.33	0.89	−3.10	...	+0.40	0.00	+0.40	−0.26	−0.74	1	Barklem et al. (2005)	
HE 0501–5139	5861	3.54	0.83	−2.38	...	+0.36	0.00	+0.36	−0.03	...	1	Barklem et al. (2005)	
HE 0501–5644	5033	2.30	1.80	−2.40	...	+0.23	+0.01	+0.24	−0.06	−0.50	1	Barklem et al. (2005)	
HE 0512–3835	4948	2.01	2.06	−2.39	...	−0.26	+0.04	−0.22	+0.13	−0.16	1	Barklem et al. (2005)	
HE 0513–4557	5629	3.62	0.68	−2.79	...	+0.35	0.00	+0.35	+0.11	...	1	Barklem et al. (2005)	
HE 0516–3820	5342	3.05	1.16	−2.32	...	+0.35	+0.01	+0.36	+0.14	−0.16	1	Barklem et al. (2005)	
HE 0517–1952	5254	1.99	2.19	−2.61	...	−0.56	+0.03	−0.53	+0.07	−0.43	1	Barklem et al. (2005)	
HE 0519–5525	5580	3.48	0.80	−2.52	...	+0.25	0.00	+0.25	+0.29	−0.24	1	Barklem et al. (2005)	
HE 0520–1748	5272	3.06	1.12	−2.52	...	+0.41	+0.01	+0.42	−0.44	−0.64	1	Barklem et al. (2005)	
HE 0524–2055	4739	1.57	2.43	−2.59	...	−0.29	+0.41	+0.12	+0.23	+0.02	1	Barklem et al. (2005)	
HE 0533–5340	4937	1.80	2.27	−2.67	...	−0.06	+0.18	+0.12	...	−0.94	1	Cohen et al. (2013)	
HE 0534–4615	5506	3.40	0.86	−2.01	...	+0.09	0.00	+0.09	+0.15	−0.06	1	Barklem et al. (2005)	
HE 0547–4539	5152	2.59	1.55	−3.01	...	+0.46	+0.01	+0.47	+0.28	−1.08	1	Barklem et al. (2005)	
HE 0557–4840	4900	2.20	1.86	−4.75	...	+1.65	+0.01	+1.66	≤ −1.04	+0.03	CEMP-no	1	Masseron et al. (2012)
HE 0858–0016	4447	0.75	3.14	−2.75	...	−0.84	+0.77	−0.07	−0.60	−0.59	1	Barklem et al. (2005)	
HE 0926–0508	6249	4.24	0.24	−2.78	...	+0.53	0.00	+0.53	+0.08	−0.36	1	Barklem et al. (2005)	
HE 0926–0546	5159	2.50	1.65	−3.73	+1.20	+0.50	+0.01	+0.51	...	−0.78	1	Cohen et al. (2013)	
HE 0938+0114	6777	4.89	−0.27	−2.51	...	+0.57	0.00	+0.57	+0.02	−0.19	1	Barklem et al. (2005)	
HE 0951–1152	5349	4.75	−0.54	−2.62	...	+0.06	0.00	+0.06	−0.40	+0.04	1	Barklem et al. (2005)	
HE 1005–1439	5202	2.55	1.61	−3.09	+1.79	+2.48	+0.02	+2.50	...	+1.17	CEMP- <i>s/rs</i>	0	Yong et al. (2013)
HE 1006–2218	6638	4.62	−0.04	−2.69	...	+0.58	0.00	+0.58	−0.05	...	1	Zhang et al. (2011)	
HE 1012–1540	5745	3.45	0.88	−3.47	+1.25	+2.22	0.00	+2.22	−0.46	−0.25	CEMP-no	1	Yong et al. (2013)
HE 1015–0027	6315	4.40	0.10	−2.65	...	+0.67	0.00	+0.67	+0.53	...	1	Zhang et al. (2011)	
HE 1031–0020	5043	2.13	1.98	−2.79	+2.48	+1.63	+0.02	+1.65	+0.39	+1.61	CEMP- <i>s/rs</i>	0	Yong et al. (2013)
HE 1044–2509	5227	2.78	1.39	−2.88	...	+0.48	+0.01	+0.49	+0.33	+0.18	1	Barklem et al. (2005)	
HE 1045+0226	5077	2.20	1.92	−2.20	...	+0.97	+0.02	+0.99	...	+1.24	CEMP- <i>s/rs</i>	0	Cohen et al. (2013)
HE 1052–2548	6534	4.52	0.04	−2.29	...	+0.47	0.00	+0.47	+0.35	+0.82	0	Barklem et al. (2005)	
HE 1054–0059	4601	1.19	2.76	−3.34	...	−0.77	+0.69	−0.08	−0.61	−1.26	1	Barklem et al. (2005)	
HE 1059–0118	5560	4.30	−0.02	−2.80	...	+0.33	0.00	+0.33	−0.41	...	1	Barklem et al. (2005)	
HE 1100–0137	6101	4.25	0.19	−2.90	...	+0.43	0.00	+0.43	1	Barklem et al. (2005)	
HE 1105+0027	6132	3.45	1.00	−2.42	...	+1.91	0.00	+1.91	+0.83	+2.36	CEMP- <i>s/rs</i>	0	Barklem et al. (2005)
HE 1111–3026	5000	2.00	2.09	−2.00	...	+0.97	+0.06	+1.03	...	+1.31	CEMP- <i>s/rs</i>	0	Cohen et al. (2013)
HE 1116–0634	4400	0.10	3.77	−3.73	...	+0.08	+0.73	+0.81	...	−1.81	CEMP-no	1	Hollek et al. (2011)
HE 1120–0153	6191	4.09	0.37	−2.77	...	+0.54	0.00	+0.54	−0.08	−0.22	1	Barklem et al. (2005)	
HE 1122–1429	5787	3.29	1.06	−2.65	...	+0.40	0.00	+0.40	+0.04	−0.40	1	Barklem et al. (2005)	
HE 1124–2335	5226	2.68	1.49	−2.95	...	+0.76	+0.01	+0.77	+0.18	−1.15	CEMP-no	1	Barklem et al. (2005)
HE 1126–1735	5689	3.31	1.01	−2.69	...	+0.19	0.00	+0.19	−0.07	−0.51	1	Barklem et al. (2005)	
HE 1127–1143	5224	2.64	1.53	−2.72	...	+0.50	+0.01	+0.51	+0.34	+0.57	1	Barklem et al. (2005)	
HE 1128–0823	5909	3.71	0.67	−2.71	...	+0.43	0.00	+0.43	+0.12	−0.21	1	Barklem et al. (2005)	
HE 1131+0141	5236	2.98	1.19	−2.49	...	+0.08	+0.01	+0.09	+0.25	+0.48	1	Barklem et al. (2005)	
HE 1132+0125	5732	3.54	0.79	−2.38	...	+0.20	0.00	+0.20	+0.07	−0.21	1	Barklem et al. (2005)	
HE 1132+0204	5046	2.25	1.86	−2.53	...	+0.09	+0.01	+0.10	−0.12	−0.74	1	Barklem et al. (2005)	

Table 3 — *Continued*

Name	T_{eff} (K)	$\log g$ (cgs)	$\log L$ (L_{\odot})	[Fe/H]	[N/Fe]	[C/Fe]	$\Delta[\text{C}/\text{Fe}]$ ([N/Fe]=0)	[C/Fe] _c	[Sr/Fe]	[Ba/Fe]	Class	I/O	Ref.
HE 1133–1641	6500	4.20	0.35	−2.82	...	+1.09	0.00	+1.09	...	−0.55	CEMP-no	1	Cohen et al. (2013)
HE 1135+0139	5487	1.80	2.45	−2.33	...	+1.11	+0.15	+1.26	+0.76	+1.04	CEMP-s/rs	0	Barklem et al. (2005)
HE 1135–0344	6154	4.03	0.42	−2.63	...	+0.99	0.00	+0.99	+0.48	...	CEMP	1	Barklem et al. (2005)
HE 1141–0610	6750	4.10	0.51	−2.28	...	+0.89	0.00	+0.89	+0.09	−0.04	CEMP-no	1	Cohen et al. (2013)
HE 1144–1349	6500	4.16	0.39	−2.61	...	+0.15	0.00	+0.15	1	Akerman et al. (2004)
HE 1148–0037	5964	4.16	0.24	−3.47	...	+0.80	0.00	+0.80	−0.32	...	CEMP	1	Barklem et al. (2005)
HE 1150–0428	5208	2.54	1.62	−3.47	+2.52	+2.37	+0.02	+2.39	−0.32	−0.48	CEMP-no	1	Yong et al. (2013)
HE 1157–0518	4900	2.00	2.06	−2.34	...	+2.15	+0.05	+2.20	...	+2.14	CEMP-s/rs	0	Aoki et al. (2007)
HE 1159–0525	4838	1.50	2.53	−2.91	...	+1.82	+0.22	+2.04	...	+1.53	CEMP-s/rs	0	Cohen et al. (2013)
HE 1201–1512	5725	3.39	0.94	−3.92	$\leq +1.29$	+1.60	0.00	+1.60	...	≤ -0.34	CEMP-no	1	Yong et al. (2013)
HE 1207–2031	6281	4.40	0.09	−2.82	...	+0.60	0.00	+0.60	−0.06	1	Barklem et al. (2005)
HE 1208–0040	5995	4.29	0.12	−2.09	...	+0.13	0.00	+0.13	1	Akerman et al. (2004)
HE 1210+0048	6028	3.73	0.69	−2.28	...	+0.48	0.00	+0.48	+0.03	−0.14	...	1	Barklem et al. (2005)
HE 1210–1956	5790	3.30	1.05	−2.57	...	+0.18	0.00	+0.18	+0.14	−0.47	...	1	Barklem et al. (2005)
HE 1212–0127	4915	1.85	2.21	−2.16	...	−0.43	+0.18	−0.25	−0.09	−0.36	...	1	Barklem et al. (2005)
HE 1214–1819	4916	1.88	2.18	−3.00	...	+0.31	+0.07	+0.38	+0.36	−0.10	...	1	Barklem et al. (2005)
HE 1215+0149	5098	2.37	1.76	−2.90	...	+0.11	+0.01	+0.12	+0.39	−0.81	...	1	Barklem et al. (2005)
HE 1217–0540	5700	4.20	0.12	−2.94	...	+0.77	0.00	+0.77	+0.23	...	CEMP	1	Barklem et al. (2005)
HE 1219–0312	5140	2.40	1.74	−2.80	...	−0.12	+0.01	−0.11	+0.41	+0.65	...	0	Barklem et al. (2005)
HE 1221–0522	5789	4.04	0.31	−2.84	...	+0.49	0.00	+0.49	−0.35	1	Barklem et al. (2005)
HE 1221–1948	6083	3.81	0.62	−3.36	...	+1.38	0.00	+1.38	CEMP	1	Barklem et al. (2005)
HE 1222–0200	5288	2.72	1.47	−2.44	...	+0.19	+0.01	+0.20	−0.03	1	Barklem et al. (2005)
HE 1222–0336	6052	3.96	0.46	−2.04	...	+0.18	0.00	+0.18	−0.23	−0.25	...	1	Barklem et al. (2005)
HE 1225+0155	4842	1.80	2.24	−2.75	...	+0.22	+0.18	+0.40	+0.18	−0.50	...	1	Barklem et al. (2005)
HE 1226–1149	5120	2.30	1.83	−2.91	+1.43	+0.42	+0.01	+0.43	...	+0.90	...	0	Cohen et al. (2013)
HE 1230–1724	5952	3.98	0.41	−2.30	...	+0.09	0.00	+0.09	+0.04	−0.22	...	1	Barklem et al. (2005)
HE 1237–3103	4851	1.72	2.32	−2.91	...	−0.10	+0.21	+0.11	−0.09	−0.65	...	1	Barklem et al. (2005)
HE 1243–1425	5507	3.19	1.07	−2.67	...	+0.47	+0.01	+0.48	+0.34	−0.45	...	1	Barklem et al. (2005)
HE 1245–0215	6500	3.80	0.75	−2.85	...	+1.66	0.00	+1.66	...	+0.29	CEMP	1	Cohen et al. (2013)
HE 1245–1616	6191	4.04	0.42	−2.98	...	+0.68	0.00	+0.68	+0.36	+0.19	...	1	Barklem et al. (2005)
HE 1246–1344	4853	1.65	2.39	−3.40	...	−0.10	+0.22	+0.12	−1.15	1	Barklem et al. (2005)
HE 1247–2114	5012	2.08	2.02	−2.61	...	+0.28	+0.02	+0.30	+0.46	−0.48	...	1	Barklem et al. (2005)
HE 1248–1800	5288	2.92	1.27	−2.89	...	+0.49	0.00	+0.49	−0.16	−0.18	...	1	Barklem et al. (2005)
HE 1249–2932	4718	1.52	2.47	−2.65	...	−0.45	+0.45	0.00	−0.78	−1.26	...	1	Barklem et al. (2005)
HE 1249–3121	5373	3.40	0.82	−3.23	...	+1.82	0.00	+1.82	−0.88	...	CEMP	1	Barklem et al. (2005)
HE 1251–0104	5084	2.32	1.80	−2.73	...	+0.21	+0.01	+0.22	−0.12	−0.42	...	1	Barklem et al. (2005)
HE 1252+0044	5296	2.98	1.21	−3.28	...	+0.50	0.00	+0.50	+0.80	−0.62	...	1	Barklem et al. (2005)
HE 1252–0117	4847	1.67	2.37	−2.86	...	−0.20	+0.27	+0.07	−0.89	−1.70	...	1	Barklem et al. (2005)
HE 1254+0009	4865	1.86	2.18	−2.95	...	−0.15	+0.08	−0.07	−0.24	−0.90	...	1	Barklem et al. (2005)
HE 1256–0228	4860	1.83	2.21	−2.08	...	−0.08	+0.19	+0.11	+0.10	+0.07	...	1	Barklem et al. (2005)
HE 1256–0651	6137	4.05	0.40	−2.36	...	+0.52	0.00	+0.52	−0.25	−0.36	...	1	Barklem et al. (2005)
HE 1258–1317	5175	2.50	1.65	−2.90	...	+0.17	+0.01	+0.18	...	−0.99	...	1	Cohen et al. (2013)
HE 1259–0621	5787	3.68	0.67	−2.64	...	+0.37	0.00	+0.37	+0.17	−0.02	...	1	Barklem et al. (2005)
HE 1300+0157	5529	3.25	1.02	−3.75	$\leq +0.71$	+1.31	0.00	+1.31	−1.73	≤ -0.85	CEMP-no	1	Yong et al. (2013)
HE 1300–0641	5308	2.96	1.24	−3.14	...	+1.20	+0.01	+1.21	−0.50	−0.86	CEMP-no	1	Barklem et al. (2005)
HE 1300–0642	5173	2.68	1.47	−3.02	...	+0.30	+0.01	+0.31	−0.12	−0.43	...	1	Barklem et al. (2005)
HE 1300–2201	6332	4.64	−0.14	−2.61	...	+0.92	0.00	+0.92	+0.38	−0.13	CEMP-no	1	Barklem et al. (2005)
HE 1300–2431	5029	1.96	2.14	−3.25	...	−0.20	+0.01	−0.19	−0.29	−0.50	...	1	Barklem et al. (2005)
HE 1305+0007	4750	2.00	2.00	−2.08	...	+1.85	+0.05	+1.90	+0.96	+2.40	CEMP-s/rs	0	Goswami et al. (2006)
HE 1305–0331	6081	4.22	0.21	−3.26	...	+1.09	0.00	+1.09	−0.07	...	CEMP	1	Barklem et al. (2005)
HE 1310–0536	4975	1.92	2.16	−4.15	$\leq +1.20$	+2.45	+0.08	+2.53	...	−0.49	CEMP-no	1	Hansen et al. (2014)
HE 1311–0131	4825	1.50	2.53	−3.15	...	+0.33	+0.40	+0.73	...	−0.62	CEMP-no	1	Hollek et al. (2011)
HE 1311–1412	4796	1.50	2.52	−2.88	...	−0.19	+0.44	+0.25	+0.04	−0.11	...	1	Barklem et al. (2005)
HE 1314–3036	4757	1.54	2.47	−2.98	...	−0.17	+0.39	+0.22	−0.02	−0.10	...	1	Barklem et al. (2005)
HE 1317–0407	4725	0.30	3.69	−3.10	...	−0.52	+0.74	+0.22	...	−0.35	...	1	Hollek et al. (2011)

Table 3 — *Continued*

Name	T_{eff} (K)	$\log g$ (cgs)	$\log L$ (L_{\odot})	[Fe/H]	[N/Fe]	[C/Fe]	$\Delta[\text{C}/\text{Fe}]$ ([N/Fe]=0)	[C/Fe] _c	[Sr/Fe]	[Ba/Fe]	Class	I/O	Ref.
HE 1319–1935	4691	1.27	2.71	−2.22	+0.46	+1.45	+0.15	+1.60	...	+1.68	CEMP- <i>s/rs</i>	0	Yong et al. (2013)
HE 1320+0139	6500	3.70	0.85	−3.38	...	+0.35	0.00	+0.35	...	−1.32		1	Cohen et al. (2013)
HE 1320–1339	4935	1.69	2.38	−2.78	...	−0.55	+0.27	−0.28	+0.33	−0.48		1	Barklem et al. (2005)
HE 1327–2326	6180	4.50	−0.04	−5.65	+4.23	+3.90	0.00	+3.90	+1.27	≤ +1.42	CEMP-no	1	Masseron et al. (2012)
HE 1330–0354	6257	4.13	0.35	−2.29	...	+0.96	0.00	+0.96	+0.11	−0.56	CEMP-no	1	Barklem et al. (2005)
HE 1330–0607	5094	2.30	1.82	−2.33	...	+0.17	+0.01	+0.18	−0.35	−0.81		1	Barklem et al. (2005)
HE 1332–0309	5125	2.40	1.73	−2.46	...	+0.17	+0.01	+0.18	+0.40	...		1	Barklem et al. (2005)
HE 1333–0340	6053	4.18	0.24	−2.64	...	+0.38	0.00	+0.38	+0.37	...		1	Zhang et al. (2011)
HE 1335+0135	5246	2.94	1.24	−2.47	...	+0.09	+0.01	+0.10	+0.14	−0.82		1	Barklem et al. (2005)
HE 1337+0012	6390	4.38	0.14	−3.25	+1.57	+0.50	0.00	+0.50	+0.28	−0.25		1	Aoki et al. (2006)
HE 1337–0453	5938	3.56	0.83	−2.34	...	+0.08	0.00	+0.08	+0.25	−0.29		1	Barklem et al. (2005)
HE 1338–0052	5856	3.70	0.67	−3.00	...	+1.32	0.00	+1.32	...	−0.02	CEMP-no	1	Cohen et al. (2013)
HE 1345–0206	5006	2.22	1.87	−2.82	...	+0.30	+0.01	+0.31	−0.33	−1.15		1	Barklem et al. (2005)
HE 1347–1025	5206	2.52	1.64	−3.71	...	+0.15	+0.01	+0.16	−1.05	−0.50		1	Yong et al. (2013)
HE 1351–1049	5204	2.85	1.31	−3.46	...	+1.46	+0.01	+1.47	+0.13	+0.05	CEMP	1	Barklem et al. (2005)
HE 1357–0123	4600	1.00	2.95	−3.80	...	−0.29	+0.69	+0.40	...	−1.69		1	Cohen et al. (2013)
HE 1405–0822	5220	1.70	2.47	−2.40	+1.34	+1.97	+0.08	+2.05	...	+1.95	CEMP- <i>s/rs</i>	0	Cui et al. (2013)
HE 1405–2512	5602	3.30	0.99	−2.80	...	+0.52	0.00	+0.52	...	−1.15		1	Cohen et al. (2013)
HE 1410+0213	5000	2.00	2.09	−2.14	+1.76	+1.71	+0.05	+1.76	...	−0.26	CEMP-no	1	Cohen et al. (2013)
HE 1410–0004	4985	2.00	2.09	−3.09	...	+2.09	+0.04	+2.13	+0.26	+1.13	CEMP- <i>s/rs</i>	0	Masseron et al. (2012)
HE 1413–1954	6533	4.59	−0.03	−3.19	...	+1.41	0.00	+1.41	−0.37	...	CEMP	1	Barklem et al. (2005)
HE 1416–1032	5000	1.80	2.29	−3.20	+0.37	−0.43	+0.09	−0.34	...	−1.24		1	Cohen et al. (2013)
HE 1419–1759	4809	1.63	2.39	−3.17	...	−0.24	+0.28	+0.04	−0.17	−0.86		1	Barklem et al. (2005)
HE 1421–2006	5687	3.73	0.59	−2.65	...	+0.26	0.00	+0.26	0.00	−0.18		1	Barklem et al. (2005)
HE 1422–0818	4816	1.30	2.73	−3.29	...	−0.14	+0.58	+0.44	...	−1.90		1	Cohen et al. (2013)
HE 1424–0241	5260	2.66	1.52	−4.05	≤ +1.13	+0.63	0.00	+0.63	≤ −1.61	−0.75		1	Yong et al. (2013)
HE 1429–0551	4757	1.39	2.62	−2.60	+1.39	+2.28	+0.10	+2.38	...	+1.47	CEMP- <i>s/rs</i>	0	Yong et al. (2013)
HE 1430–0026	5855	4.12	0.25	−2.78	...	+0.48	0.00	+0.48	−0.12	−0.31		1	Barklem et al. (2005)
HE 1430–1123	5915	3.75	0.63	−2.71	...	+1.75	0.00	+1.75	+0.34	+1.73	CEMP- <i>s/rs</i>	0	Barklem et al. (2005)
HE 1431–2142	6137	4.10	0.35	−2.60	...	+0.44	0.00	+0.44	+0.07	+0.08		1	Barklem et al. (2005)
HE 1432–1819	5975	3.60	0.80	−2.56	...	+0.83	0.00	+0.83	...	−0.67	CEMP-no	1	Cohen et al. (2013)
HE 1434–1442	5420	3.20	1.03	−2.39	+1.70	+1.95	+0.01	+1.96	...	+1.23	CEMP- <i>s/rs</i>	0	Cohen et al. (2013)
HE 1439–0218	6150	3.70	0.75	−2.65	...	+0.66	0.00	+0.66	...	−0.15		1	Cohen et al. (2013)
HE 1439–1420	6056	3.80	0.62	−2.97	+1.09	+1.84	0.00	+1.84	...	+1.31	CEMP- <i>s/rs</i>	0	Cohen et al. (2013)
HE 1443+0113	5000	2.00	2.09	−2.11	...	+1.52	+0.06	+1.58	...	+1.79	CEMP- <i>s/rs</i>	0	Cohen et al. (2013)
HE 1446–0140	6090	4.40	0.03	−2.38	...	+0.14	0.00	+0.14	...	−0.16		1	Cohen et al. (2013)
HE 1447+0102	5100	1.70	2.43	−2.47	...	+2.48	+0.06	+2.54	...	+2.70	CEMP- <i>s/rs</i>	0	Aoki et al. (2007)
HE 1456+0230	5664	2.20	2.11	−3.32	+2.84	+2.14	+0.02	+2.16	...	−0.19	CEMP-no	1	Cohen et al. (2013)
HE 1500–1628	4807	1.50	2.52	−2.38	...	−0.01	+0.48	+0.47	−1.66	−1.72		1	Cohen et al. (2013)
HE 1506–0113	5016	2.01	2.09	−3.54	+0.61	+1.47	+0.02	+1.49	...	−0.80	CEMP-no	1	Yong et al. (2013)
HE 1509–0806	5185	2.50	1.65	−2.91	+2.23	+1.98	+0.02	+2.00	+1.20	+1.93	CEMP- <i>s/rs</i>	0	Cohen et al. (2013)
HE 1523–1155	4800	1.60	2.42	−2.15	...	+1.86	+0.07	+1.93	...	+1.72	CEMP- <i>s/rs</i>	0	Aoki et al. (2007)
HE 1528–0409	5000	1.80	2.29	−2.60	...	+2.41	+0.06	+2.47	...	+2.30	CEMP- <i>s/rs</i>	0	Aoki et al. (2007)
HE 2122–4707	5147	2.50	1.64	−2.42	...	+1.60	+0.02	+1.62	...	+2.03	CEMP- <i>s/rs</i>	0	Cohen et al. (2013)
HE 2123–0329	4725	1.15	2.84	−3.22	...	+0.40	+0.66	+1.06	...	−0.85	CEMP-no	1	Hollek et al. (2011)
HE 2133–1426	6300	4.10	0.39	−3.32	+1.62	+1.79	0.00	+1.79	−0.15	+2.34	CEMP- <i>s/rs</i>	0	Cohen et al. (2013)
HE 2133–1432	5716	3.46	0.86	−2.02	...	+0.08	0.00	+0.08	+0.21	−0.10		1	Barklem et al. (2005)
HE 2134+0001	5257	3.00	1.18	−2.22	...	+0.16	+0.01	+0.17	+0.02	−0.47		1	Barklem et al. (2005)
HE 2138–0314	5015	1.90	2.20	−3.29	...	+0.78	+0.04	+0.82	...	−0.85	CEMP-no	1	Hollek et al. (2011)
HE 2138–3336	5850	3.60	0.76	−2.79	+1.66	+2.43	0.00	+2.43	+0.27	+1.91	CEMP- <i>s/rs</i>	0	Placco et al. (2013)
HE 2139–1851	4925	1.86	2.21	−3.24	...	+0.45	+0.05	+0.50	+0.39	−0.95		1	Barklem et al. (2005)
HE 2139–5432	5416	3.04	1.19	−4.02	+2.08	+2.59	+0.01	+2.60	...	≤ −0.33	CEMP-no	1	Yong et al. (2013)
HE 2141–3741	4945	1.00	3.07	−3.30	+1.37	+0.07	+0.76	+0.83	−0.57	−1.28	CEMP-no	1	Placco et al. (2014a)
HE 2142–5656	4939	1.85	2.22	−2.87	+0.54	+0.95	+0.10	+1.05	...	−0.63	CEMP-no	1	Yong et al. (2013)
HE 2143+0030	4688	1.50	2.48	−2.43	...	−0.40	+0.50	+0.10	+0.01	−0.43		1	Barklem et al. (2005)

Table 3 — *Continued*

Name	T_{eff} (K)	$\log g$ (cgs)	$\log L$ (L_{\odot})	[Fe/H]	[N/Fe]	[C/Fe]	$\Delta[\text{C}/\text{Fe}]$ ([N/Fe]=0)	$[\text{C}/\text{Fe}]_c$	[Sr/Fe]	[Ba/Fe]	Class	I/O	Ref.
HE 2145–3025	5608	2.22	2.07	−2.69	...	−0.24	+0.01	−0.23	+0.56	−0.36		1	Barklem et al. (2005)
HE 2148–1105a	4400	0.20	3.67	−2.98	...	−0.42	+0.75	+0.33	...	−1.09		1	Hollek et al. (2011)
HE 2148–1247	6380	3.90	0.62	−2.30	...	+1.70	0.00	+1.70	+0.84	+1.92	CEMP-s/rs	0	Cohen et al. (2013)
HE 2151–2858	5598	4.14	0.15	−2.38	...	+0.06	0.00	+0.06	−0.18	−0.30		1	Barklem et al. (2005)
HE 2153–2719	4898	2.01	2.05	−2.49	...	+0.08	+0.03	+0.11	+0.10	−0.74		1	Barklem et al. (2005)
HE 2155+0136	5331	3.22	0.98	−2.07	...	−0.04	0.00	−0.04	−0.02	+0.09		1	Barklem et al. (2005)
HE 2155–3750	5000	2.30	1.79	−2.59	+1.48	+1.78	+0.02	+1.80	...	+1.73	CEMP-s/rs	0	Cohen et al. (2013)
HE 2156–3130	4692	1.28	2.70	−3.13	...	+0.65	+0.54	+1.19	−0.80	+0.43	CEMP	1	Barklem et al. (2005)
HE 2157–3404	4990	1.30	2.79	−2.89	+0.66	−0.54	+0.62	+0.08	−0.48	−1.39		1	Placco et al. (2014a)
HE 2158–0348	5150	2.44	1.70	−2.57	+1.52	+1.87	+0.02	+1.89	+0.60	+1.75	CEMP-s/rs	0	Yong et al. (2013)
HE 2200–1946	5000	2.50	1.59	−2.63	...	+0.34	+0.01	+0.35	...	−1.43		1	Cohen et al. (2013)
HE 2200–2030	5870	3.42	0.95	−2.00	...	+0.06	0.00	+0.06	+0.03	−0.09		1	Barklem et al. (2005)
HE 2201–0637	4976	2.21	1.87	−2.59	...	+0.10	+0.01	+0.11	0.00	−0.72		1	Barklem et al. (2005)
HE 2202–4831	5331	2.95	1.25	−2.78	...	+2.41	+0.02	+2.43	...	−1.28	CEMP-no	1	Yong et al. (2013)
HE 2203–3723	5118	2.20	1.93	−3.30	...	+1.00	+0.01	+1.01	...	−0.24	CEMP-no	1	Cohen et al. (2013)
HE 2204–1703	4932	1.87	2.20	−2.79	...	+0.17	+0.11	+0.28	−0.43	−0.80		1	Barklem et al. (2005)
HE 2206–2245	5100	2.45	1.68	−2.73	...	+0.17	+0.01	+0.18	+0.05	−0.16		1	Barklem et al. (2005)
HE 2215–2548	5035	2.10	2.00	−3.01	...	+0.18	+0.01	+0.19	...	−0.95		1	Cohen et al. (2013)
HE 2216–0621	4671	1.27	2.70	−3.23	...	−0.70	+0.62	−0.08	−0.39	−1.31		1	Barklem et al. (2005)
HE 2217–0706	4497	1.01	2.90	−2.58	...	−0.59	+0.75	+0.16	−0.09	−0.61		1	Barklem et al. (2005)
HE 2217–1523	4847	1.82	2.22	−2.62	...	0.00	+0.17	+0.17	−0.05	−0.57		1	Barklem et al. (2005)
HE 2217–4053	5148	2.40	1.74	−3.37	+0.65	+1.14	+0.01	+1.15	...	+1.30	CEMP-s/rs	0	Cohen et al. (2013)
HE 2219–0713	4789	1.68	2.34	−2.92	...	−0.21	+0.25	+0.04	−0.22	−1.41		1	Barklem et al. (2005)
HE 2221–0453	4430	0.73	3.15	−2.00	+0.84	+1.83	+0.08	+1.91	...	+1.76	CEMP-s/rs	0	Yong et al. (2013)
HE 2221–4150	5887	4.06	0.32	−2.03	...	+0.19	0.00	+0.19	+0.12	+0.04		1	Barklem et al. (2005)
HE 2222–4156	5537	3.27	1.00	−2.73	...	+0.38	0.00	+0.38	+0.16	−0.21		1	Barklem et al. (2005)
HE 2224+0143	5198	2.66	1.50	−2.58	...	+0.31	+0.01	+0.32	+0.33	+0.53		1	Barklem et al. (2005)
HE 2224–4103	5074	2.32	1.80	−2.60	...	+0.19	+0.01	+0.20	−0.00	−0.62		1	Barklem et al. (2005)
HE 2226–4102	5140	2.43	1.71	−2.87	...	+0.42	+0.01	+0.43	+0.05	−1.05		1	Barklem et al. (2005)
HE 2227–4044	5811	3.85	0.50	−2.32	...	+1.59	0.00	+1.59	+0.51	+1.29	CEMP-s/rs	0	Barklem et al. (2005)
HE 2228–0706	5003	2.02	2.07	−2.78	+1.13	+2.32	+0.04	+2.36	...	+2.46	CEMP-s/rs	0	Yong et al. (2013)
HE 2228–3806	5175	2.62	1.53	−3.07	...	+0.38	+0.01	+0.39	−0.09	−0.62		1	Barklem et al. (2005)
HE 2229–4153	5138	2.47	1.67	−2.59	...	+0.33	+0.01	+0.34	+0.19	−0.33		1	Barklem et al. (2005)
HE 2231–0622	5211	2.90	1.26	−2.12	...	−0.12	+0.01	−0.11	−0.40	−0.51		1	Barklem et al. (2005)
HE 2233–4724	4360	0.40	3.45	−3.65	...	−0.48	+0.70	+0.22	−0.77	−1.13		1	Placco et al. (2014a)
HE 2234–0521	5332	3.15	1.05	−2.78	...	+0.32	+0.01	+0.33	−0.20	−0.89		1	Barklem et al. (2005)
HE 2236+0204	5036	2.10	2.00	−2.86	...	+0.22	+0.01	+0.23	...	−0.05		1	Cohen et al. (2013)
HE 2238–0131	4350	0.15	3.70	−3.00	...	−0.42	+0.75	+0.33	...	−0.46		1	Hollek et al. (2011)
HE 2238–2152	5427	3.28	0.95	−2.40	...	+0.09	0.00	+0.09	−0.19	−0.42		1	Barklem et al. (2005)
HE 2239–5019	6125	3.48	0.96	−4.15	$\leq +1.20$	+1.80	0.00	+1.80	...	≤ 0.00	CEMP-no	1	Hansen et al. (2014)
HE 2240–0412	5852	4.33	0.04	−2.20	...	+1.26	0.00	+1.26	+0.34	+1.28	CEMP-s/rs	0	Barklem et al. (2005)
HE 2242–1930	5281	2.99	1.20	−2.21	...	+0.05	+0.01	+0.06	+0.06	−0.15		1	Barklem et al. (2005)
HE 2244–1503	5122	2.57	1.56	−2.87	...	+0.11	+0.01	+0.12	−0.10	+0.40		1	Barklem et al. (2005)
HE 2244–2116	5230	2.70	1.47	−2.35	...	−0.35	+0.01	−0.34	...	−1.92		1	Cohen et al. (2013)
HE 2247–3705	5366	3.04	1.17	−2.26	...	+0.32	+0.01	+0.33	−0.23	−0.88		1	Barklem et al. (2005)
HE 2247–7400	4829	1.56	2.47	−2.87	...	+0.70	+0.32	+1.02	...	−0.94	CEMP-no	1	Yong et al. (2013)
HE 2248–3345	5011	2.11	1.99	−2.73	...	+0.17	+0.01	+0.18	−1.89	−1.42		1	Barklem et al. (2005)
HE 2249–1704	4592	1.10	2.84	−2.95	...	+1.76	+0.31	+2.07	...	+1.75	CEMP-s/rs	0	Cohen et al. (2013)
HE 2250–2132	5705	3.69	0.63	−2.22	...	+0.37	0.00	+0.37	+0.10	−0.36		1	Barklem et al. (2005)
HE 2251–0821	5160	2.50	1.65	−2.91	...	+0.57	+0.01	+0.58	...	−0.49		1	Cohen et al. (2013)
HE 2252–4225	4708	1.53	2.46	−2.82	...	−0.43	+0.43	0.00	+0.16	+0.40		1	Barklem et al. (2005)
HE 2253–0849	4425	0.20	3.68	−2.88	...	−0.77	+0.76	−0.01	...	−0.38		1	Hollek et al. (2011)
HE 2258–3456	4988	1.55	2.54	−2.97	...	−0.24	+0.39	+0.15	−0.93	−1.20		1	Barklem et al. (2005)
HE 2258–6358	4900	1.60	2.46	−2.67	+1.44	+2.42	+0.08	+2.50	+0.80	+2.23	CEMP-s/rs	0	Placco et al. (2013)
HE 2259–3407	6266	4.32	0.16	−2.29	...	+0.37	0.00	+0.37	−0.08	−0.57		1	Barklem et al. (2005)

Table 3 — *Continued*

Name	T_{eff} (K)	$\log g$ (cgs)	$\log L$ (L_{\odot})	[Fe/H]	[N/Fe]	[C/Fe]	$\Delta[\text{C}/\text{Fe}]$ ([N/Fe]=0)	$[\text{C}/\text{Fe}]_c$	[Sr/Fe]	[Ba/Fe]	Class	I/O	Ref.
HE 2301–4024	5743	3.76	0.57	−2.10	...	+0.26	0.00	+0.26	+0.10	+0.44		1	Barklem et al. (2005)
HE 2301–4126	5841	3.66	0.70	−2.37	...	+0.35	0.00	+0.35	+0.03	+0.06		1	Barklem et al. (2005)
HE 2302–2154a	4675	0.90	3.08	−3.90	...	+0.38	+0.70	+1.08	...	−1.50	CEMP-no	1	Hollek et al. (2011)
HE 2304–4153	4663	1.01	2.96	−3.02	...	−0.69	+0.75	+0.06	−1.53	−1.66		1	Barklem et al. (2005)
HE 2311+0129	5188	2.65	1.51	−2.78	...	+0.29	+0.01	+0.30	+0.20	−0.24		1	Barklem et al. (2005)
HE 2314–1554	5050	2.20	1.91	−3.28	+2.20	+1.01	+0.01	+1.02	+0.16	−0.77	CEMP-no	1	Cohen et al. (2013)
HE 2318–1621	4846	1.40	2.64	−3.67	+1.24	+1.04	+0.50	+1.54	−1.00	−1.61	CEMP-no	1	Placco et al. (2014a)
HE 2319–0852	4724	1.36	2.63	−3.38	...	−0.36	+0.52	+0.16	−0.43	−1.04		1	Barklem et al. (2005)
HE 2323–0256	4958	1.84	2.24	−3.97	+2.16	+1.06	+0.04	+1.10	...	−0.52	CEMP-no	1	Yong et al. (2013)
HE 2323–6549	5215	2.60	1.56	−3.35	+0.42	+0.72	+0.01	+0.73	+0.03	−0.58	CEMP-no	1	Placco et al. (2014a)
HE 2325–0755	5663	3.17	1.14	−2.85	...	+0.17	0.00	+0.17	−0.14	−0.62		1	Barklem et al. (2005)
HE 2326+0038	5145	2.51	1.63	−2.78	...	+0.19	+0.01	+0.20	−0.35	−0.71		1	Barklem et al. (2005)
HE 2327–5642	5050	2.34	1.77	−2.78	−0.20	+0.13	+0.01	+0.14	+0.40	+0.31		1	Masseron et al. (2010)
HE 2329–3702	6060	3.72	0.71	−2.15	...	+0.11	0.00	+0.11	+0.24	−0.19		1	Barklem et al. (2005)
HE 2330–0555	4867	1.65	2.40	−2.98	+1.00	+2.09	+0.15	+2.24	...	+1.17	CEMP-s/rs	0	Yong et al. (2013)
HE 2333–1358	5020	2.15	1.95	−3.34	...	+0.29	+0.01	+0.30	−1.77	...		1	Barklem et al. (2005)
HE 2335–5958	5765	3.24	1.10	−2.32	...	+0.04	0.00	+0.04	+0.05	−0.37		1	Barklem et al. (2005)
HE 2338–1311	5582	3.50	0.78	−2.86	...	+0.30	0.00	+0.30		1	Barklem et al. (2005)
HE 2338–1618	5515	3.38	0.88	−2.64	...	+0.43	0.00	+0.43	−0.12	...		1	Barklem et al. (2005)
HE 2341–2029	6500	4.40	0.15	−2.53	+1.10	+1.05	0.00	+1.05	−0.01	−0.42	CEMP-no	1	Cohen et al. (2013)
HE 2345–1919	5617	4.46	−0.17	−2.46	...	+0.20	0.00	+0.20	−0.18	−0.51		1	Barklem et al. (2005)
HE 2347–1334	4453	0.95	2.94	−2.56	...	−0.54	+0.75	+0.21	−0.11	−0.83		1	Barklem et al. (2005)
HE 2347–1448	6162	3.98	0.47	−2.31	...	+0.46	0.00	+0.46	+0.18	−0.21		1	Barklem et al. (2005)
HE 2356–0410	5170	2.45	1.70	−3.19	+1.75	+2.27	+0.02	+2.29	−0.90	−0.80	CEMP-no	1	Yong et al. (2013)
HE 2357–0701	5142	2.40	1.74	−3.17	+0.87	+0.26	+0.01	+0.27	...	−1.34		1	Cohen et al. (2013)
HK17435–00532	5200	2.15	2.01	−2.23	...	+0.77	+0.01	+0.78	+0.41	+0.86	CEMP	0	Roederer et al. (2008b)
LP625–44	5500	2.80	1.46	−2.71	+1.00	+2.10	+0.02	+2.12	+1.22	+2.74	CEMP-s/rs	0	Masseron et al. (2012)
LP 815–43	6533	4.25	0.31	−2.67	...	+0.22	0.00	+0.22	−0.01	...		1	Akerman et al. (2004)
SDSS J0002+29	6150	4.00	0.45	−3.26	...	+2.63	0.00	+2.63	...	+1.84	CEMP-s/rs	0	Aoki et al. (2013)
SDSS J0018–09	4600	5.00	−1.05	−2.65	...	−0.88	0.00	−0.88		1	Aoki et al. (2013)
SDSS J0036–10	6479	4.31	0.23	−2.60	...	+2.32	0.00	+2.32	...	+0.40	CEMP	1	Yong et al. (2013)
SDSS J0126+06	6900	4.00	0.65	−3.01	...	+3.08	0.00	+3.08	...	+3.20	CEMP-s/rs	0	Aoki et al. (2013)
SDSS J0140+23	5703	3.36	0.96	−4.09	...	+1.57	0.00	+1.57	...	≤ −0.04	CEMP-no	1	Yong et al. (2013)
SDSS J0259+00	4550	5.00	−1.07	−3.31	...	−0.02	0.00	−0.02		1	Aoki et al. (2013)
SDSS J0308+05	5950	4.00	0.39	−2.19	...	+2.36	0.00	+2.36	CEMP	1	Aoki et al. (2013)
SDSS J0351+10	5450	3.60	0.64	−3.18	...	+1.55	0.00	+1.55	CEMP-no	1	Aoki et al. (2013)
SDSS J0629+83	5550	4.00	0.27	−2.82	...	+2.09	0.00	+2.09	CEMP	1	Aoki et al. (2013)
SDSS J0711+67	5350	3.00	1.21	−2.91	...	+1.98	+0.01	+1.99	...	+0.82	CEMP	0	Aoki et al. (2013)
SDSS J0723+36	5150	2.20	1.94	−3.32	...	+1.79	+0.02	+1.81	CEMP-no	1	Aoki et al. (2013)
SDSS J0741+67	5200	2.50	1.66	−2.87	...	+0.74	+0.01	+0.75	...	+0.26	CEMP	1	Aoki et al. (2013)
SDSS J0817+26	6300	4.00	0.49	−3.16	...	+2.41	0.00	+2.41	...	+0.77	CEMP	0	Aoki et al. (2008)
SDSS J0858+35	5200	2.50	1.66	−2.53	...	+0.30	+0.01	+0.31	...	−0.02		1	Aoki et al. (2013)
SDSS J0912+02	6500	4.50	0.05	−2.50	+1.75	+2.17	0.00	+2.17	...	+1.49	CEMP-s/rs	0	Masseron et al. (2012)
SDSS J0918+37	6463	4.34	0.20	−2.98	...	+2.82	0.00	+2.82	...	+1.70	CEMP-s/rs	0	Yong et al. (2013)
SDSS J0924+40	6196	3.77	0.69	−2.68	...	+2.72	0.00	+2.72	...	+1.73	CEMP-s/rs	0	Yong et al. (2013)
SDSS J1029+17	5811	4.00	0.35	−4.99	≤ +0.20	+0.70	0.00	+0.70	CEMP	1	Caffau et al. (2011)
SDSS J1036+12	6000	4.00	0.41	−3.20	+1.29	+1.47	0.00	+1.47	...	+1.17	CEMP-s/rs	0	Masseron et al. (2012)
SDSS J1114+18	6200	4.00	0.47	−3.35	...	+3.25	0.00	+3.25	...	+1.62	CEMP-s/rs	0	Spite et al. (2013)
SDSS J1143+20	6240	4.00	0.48	−3.15	...	+2.75	0.00	+2.75	...	+1.84	CEMP-s/rs	0	Spite et al. (2013)
SDSS J1241–08	5150	2.50	1.64	−2.73	...	+0.50	+0.01	+0.51	...	−0.45		1	Aoki et al. (2013)
SDSS J1242–03	5150	2.50	1.64	−2.77	...	+0.64	+0.01	+0.65	...	−0.11		1	Aoki et al. (2013)
SDSS J1245–07	6100	4.00	0.44	−3.17	...	+2.53	0.00	+2.53	...	+2.09	CEMP-s/rs	0	Aoki et al. (2013)
SDSS J1349–02	6200	4.00	0.47	−3.00	+1.60	+2.82	0.00	+2.82	...	+2.17	CEMP-s/rs	0	Masseron et al. (2012)
SDSS J1422+00	5200	2.20	1.96	−3.03	...	+1.70	+0.01	+1.71	...	−1.18	CEMP-no	1	Aoki et al. (2013)
SDSS J1612+04	5350	3.30	0.91	−2.86	...	+0.63	0.00	+0.63	...	+0.05		1	Aoki et al. (2013)

Table 3 — *Continued*

Name	T_{eff} (K)	$\log g$ (cgs)	$\log L$ (L_{\odot})	[Fe/H]	[N/Fe]	[C/Fe]	$\Delta[\text{C}/\text{Fe}]$ ([N/Fe]=0)	[C/Fe] _c	[Sr/Fe]	[Ba/Fe]	Class	I/O	Ref.
SDSS J1613+53	5350	2.10	2.11	-3.33	...	+2.09	+0.02	+2.11	...	+0.03	CEMP	1	Aoki et al. (2013)
SDSS J1626+14	6400	4.00	0.52	-2.99	...	+2.86	0.00	+2.86	...	+1.69	CEMP-s/rs	0	Aoki et al. (2013)
SDSS J1646+28	6100	4.00	0.44	-3.05	...	+2.52	0.00	+2.52	...	+1.78	CEMP-s/rs	0	Aoki et al. (2013)
SDSS J1703+28	5100	4.80	-0.67	-3.21	...	+0.28	0.00	+0.28		1	Aoki et al. (2013)
SDSS J1707+58	6700	4.20	0.40	-2.52	...	+2.14	0.00	+2.14	...	+3.40	CEMP-s/rs	0	Aoki et al. (2008)
SDSS J1734+43	5200	2.70	1.46	-2.51	...	+1.78	+0.02	+1.80	...	+1.61	CEMP-s/rs	0	Aoki et al. (2013)
SDSS J1746+24	5350	2.60	1.61	-3.17	...	+1.24	+0.01	+1.25	...	+0.26	CEMP	1	Aoki et al. (2013)
SDSS J1836+63	5350	3.00	1.21	-2.85	...	+2.02	+0.01	+2.03	...	+2.37	CEMP-s/rs	0	Aoki et al. (2013)
SDSS J2047+00	6383	4.36	0.16	-2.36	...	+2.00	0.00	+2.00	...	+1.70	CEMP-s/rs	0	Yong et al. (2013)
SDSS J2206-09	5100	2.10	2.03	-3.17	...	+0.64	+0.01	+0.65	...	-0.85		1	Aoki et al. (2013)
SDSS J2209-00	6440	4.00	0.53	-4.00	...	+2.56	0.00	+2.56	...	$\leq +1.05$	CEMP-no	1	Spite et al. (2013)
SDSS J2357-00	5200	4.80	-0.64	-3.20	...	+0.57	0.00	+0.57	...	+1.33		0	Aoki et al. (2013)

Note. — Class column:

CEMP: $[\text{C}/\text{Fe}] \geq +0.7$

CEMP-no: $[\text{C}/\text{Fe}] \geq +0.7$ and $[\text{Ba}/\text{Fe}] \leq 0.0$, or a published light-element enrichment pattern that clearly suggests CEMP-no status.

CEMP-s/rs: $[\text{C}/\text{Fe}] \geq +0.7$ and $[\text{Ba}/\text{Fe}] \geq 1.0$

I/O rejection flag:

“1” for accepted stars ($[\text{Ba}/\text{Fe}] < +0.6$, $[\text{Ba}/\text{Sr}] < 0.0$, and upper limits for $[\text{Ba}/\text{Fe}]$)

“0” for stars rejected on the CEMP-star frequency calculations ($[\text{Ba}/\text{Fe}] > +1.0$ and $[\text{Ba}/\text{Sr}] > 0.0$)